Joint impact on thermotolerance of yeast species divergence in mitochondrial and nuclear genomes

Jun-Ting Johnson Wang[1,2], Priscilla Ng[1,3], Maceo E. Powers[1,4], Rachel B. Brem[1*]

[1]Department of Plant and Microbial Biology, University of California, Berkeley, Berkeley, CA, 94720

[2]Graduate Group in Comparative Biochemistry, University of California, Berkeley, Berkeley, CA, 94720

[3]Current address: BillionToOne, Menlo Park, CA, 94025

[4]Current address: Laboratory of Viral Diseases, National Institute of Allergy and Infectious Diseases, National Institutes of Health, Bethesda, MD, 20892

*To whom correspondence should be addressed (rbrem@berkeley.edu)

Abstract

Many traits of interest in biology evolved long ago and are fixed in a particular species, distinguishing it from other sister taxa. Elucidating the mechanisms underlying such ancient traits has been a central goal for evolutionary biologists. The yeast *Saccharomyces cerevisiae* is unique among its relatives for its ability to thrive at high temperature. The genetic determinants of the trait remain incompletely understood. We sought to understand the contribution of species variation in mitochondrial DNA to yeast thermotolerance. We used mitochondrial transgenesis to show that *S. cerevisiae* mitotypes were sufficient for a partial boost to thermotolerance and respiration in the *S. paradoxus* background. These mitochondrial alleles worked best when the background also harbored a pro-thermotolerance nuclear genotype, attesting to positive epistasis between the two genomes. The benefits of *S. cerevisiae* alleles in terms of respiration and growth at high temperature came at the cost of worse performance in cooler conditions. Together, our results establish this system as a case in which mitoalleles have fitness benefits and work well in multiple backgrounds; given the high mutation rate of the mitochondrial compartment, they were also likely extra easy for the ancestral population to acquire. We thus propose a broader model in which mitochondrial variants may prove to be especially good candidates in the search for genetic mechanisms of the adaptive process.

Introduction

A central aim in evolutionary genetics is to figure out how organisms acquire new traits. In the study of within-species variation, a rich literature has provided insights into the mechanisms of local adaptation in the wild (Elena 2017; Kraemer and Boynton 2017; Sork 2017; Rees et al. 2020; Bazzicalupo 2022). Yet many characters of basic and applied interest evolved long ago and are fixed in a particular species, distinguishing it from unaffected relatives. Against a backdrop of years of genomic and experimental pursuit (Allen Orr 2001; Nikolov and Tsiantis 2015; Weiss and Brem 2019), as a field we still know surprisingly little about how evolution engineers and refines phenotypes over long timescales, with the widest knowledge gap in the case of polygenic architectures. Shedding light on these processes, by dissecting the genetics of ancient traits, remains a key challenge for the field.

Sequence variants in mitotype, the DNA of the mitochondrial organelle, have emerged as an important part of the genetic architecture of naturally varying traits. Mitotype variants have been directly implicated in trait innovation, both independently and in concert with nuclear genomes (Melvin and Ballard 2006; Tranah 2011; Houtkooper et al. 2013; Sullivan and Chandel 2014; Sun et al. 2019; Cao et al. 2022; Meng et al. 2022; Oppong et al. 2022; Quéméneur et al. 2022; Parra et al. 2023; Moran et al. 2024). Though small in length, the mitochondrial genome has the potential for an outsize influence on trait variation, given its increased mutation rate and large mutational target of the multi-copy mitochondrial genome relative to nuclear chromosomes (Pakendorf and Stoneking 2005; Chou and Leu 2015; Ferreira and Rodriguez 2024).

Saccharomyces budding yeasts diverged from a common ancestor ~20 million years ago (Kellis et al. 2003) and have served for decades as a model for the study of interspecific trait variation, including in metabolism, genome content, cell cycle, and reproductive isolation (Hou et al. 2014; Roop et al. 2016; Bozdag et al. 2021; Fredericks et al. 2021; Lupo et al. 2021; Marsit et al. 2021; Smukowski Heil et al. 2021; Swamy et al. 2022; Crandall et al. 2023; Forejt and Jansa 2023; Peris et al. 2023). A long-standing subset of this field has focused on species-unique traits driven by mitochondrial genomes (Sulo et al. 2003; Wolff et al. 2014; De Chiara et al. 2020; Hewitt et al. 2020; Hénault et al. 2022), with particularly detailed mechanistic validation in studies of speciation (Lee et al. 2008; Chou et al. 2010; Mário et al. 2015; Jhuang et al. 2017) (complementing studies of within-species mitotype variation (Wolters et al. 2015; Leducq et al.

2017; Wolters et al. 2018; Vijayraghavan et al. 2019; Vijayraghavan et al. 2019; Nguyen et al. 2020)). A key model trait in the *Saccharomyces* system is temperature preference, as the best-studied yeast species, *S. cerevisiae,* is unique within the *Saccharomyces* clade for its ability to thrive at high temperature (Sweeney et al. 2004; Gonçalves et al. 2011; Salvadó et al. 2011), whereas others in the clade exhibit cryotolerance (Paget et al. 2014; Pinto et al. 2025). A growing literature has implicated nuclear loci in species differences in thermotolerance (Weiss et al. 2018; AlZaben et al. 2021; Walunjkar et al. 2024) and cold tolerance (Paget et al. 2014; Pinto et al. 2025). The contribution of mitochondrial genome variation to this trait has also been suggested, based on analyses of interspecies hybrids (Baker et al. 2019; Li et al. 2019; Hewitt et al. 2020); exactly what the divergent mitotypes of *Saccharomyces* species do phenotypically, and how they exert their effects, remains incompletely understood.

We set out to deepen our understanding of the phenotypic impact of mitochondrial variation between *Saccharomyces* species, both in isolation and in conjunction with nuclear loci. We anticipated that our findings would further illuminate the mechanisms of thermotolerance and their evolutionary history. We designed an approach that used *S. paradoxus*, a relatively thermosensitive species sister to *S. cerevisiae,* as a model for the common ancestor on whose background traits would have arisen as the two species diverged. We manipulated the nuclear and mitochondrial genome in this system to investigate their contributions to metabolism and thermotolerance.

Results

S. cerevisiae* mitotypes are sufficient to heighten respiratory behaviors in *S. paradoxus

Previous studies have used yeast interspecies hybrids to establish an association between *S. cerevisiae* mitochondrial alleles and thermotolerance (Baker et al. 2019; Li et al. 2019; Hewitt et al. 2020), which parallels the advantage of *S. cerevisiae* purebreds at high temperature, relative to other species in the clade. We reasoned that investigating mitotype genetics in purebred *S. paradoxus* could help shed additional light on the mechanisms of evolutionary innovation along the *S. cerevisiae* lineage. For this purpose, we developed a series of cybrids, in which we introduced each mitochondrial genome in turn from a suite of *S. cerevisiae* isolates from different geographical locations, which all grew well in standard conditions and at high temperature (Figure S1), into a tester strain of *S. paradoxus*, the English oak tree isolate Z1 (Figure 1). Since they lack the endogenous *S. paradoxus* mitotype, these strains represented an experimental resource for the study of the phenotypic impact of *S. cerevisiae* mitochondrial alleles in an isogenic background, and they were viable and stable as expected (Sulo et al. 2003; Mário et al. 2015).

Before using our cybrids to address thermotolerance *per se*, we first investigated the hypothesis that respiration, as a proximal function of the mitochondrion and its genome, would be perturbed by species variation in mitotype. Wild-type *S. cerevisiae* strains as a rule grow better than those of *S. paradoxus* on glycerol, a non-fermentable carbon source (Figure S2), and in interspecies hybrid backgrounds, *S. cerevisiae* mitotypes promote growth in this condition (Li et al. 2019). To explore the impact of *S. cerevisiae* mitochondrial DNA alleles on respiratory growth in a purebred context, we subjected our cybrids to the liquid growth assay in glycerol media. The results revealed robust improvement in glycerol growth attributable to *S. cerevisiae* mitotypes in the *S. paradoxus* background, for three of our *S. cerevisiae* donors (Figure 2A). The fourth cybrid, harboring mitochondrial DNA from the *S. cerevisiae* vineyard isolate Y55, had a defect in growth on glycerol (Figure 2A), which echoes previously reported incompatibilities of this mitotype in other backgrounds (Wolters et al. 2018). Together, these data suggested that pro-

104 respiratory effects could be a prevalent characteristic of mitochondrial genomes from across the
105 *S. cerevisiae* population.

106 As a more direct measure of metabolic effects driven by *S. cerevisiae* mitochondria DNA, we
107 established an assay of reduction of the colorimetric substrate 1-(4,5-dimethylthiazol-2-yl)-3,5-
108 diphenyltetrazolium bromide (MTT) in glucose medium. This signal serves as a reporter of
109 activities of the electron transport chain, particularly succinate dehydrogenase (Slater et al.
110 1963; Sánchez and Königsberg 2006; Jain et al. 2018) (though see (Shoemaker et al. 2004)
111 and (Peng et al. 2005)), and thus is informative as a marker of respiration. A first set of
112 observations revealed no detectable impact of mitotype on MTT reduction during culture in
113 liquid glucose medium at 28°C, in our cybrids in the Z1 *S. paradoxus* background (Figure 3A).
114 We reasoned that the metabolic effect of *S. cerevisiae* mitotypes might be better resolved at
115 higher temperatures, in which yeast cells respire particularly avidly (Rikhvanov et al. 2001).
116 Consistent with this notion, in culture at 39°C in glucose medium, we observed increased MTT
117 reduction in all cybrids except for that harboring *S. cerevisiae* Y55 mitochondrial DNA, relative
118 to wild-type Z1 *S. paradoxus* with its endogenous mitochondrial genome (Figure 3B). Together,
119 these results established that in the *S. paradoxus* background, *S. cerevisiae* mitotypes can be
120 sufficient for increased growth and metabolic behaviors that are signatures of respiration.

121 **_S. cerevisiae_ mitotypes boost thermotolerance in _S. paradoxus_**

122 We now turned to high-temperature growth proper, as an additional phenotype that we
123 hypothesized would be modulated by mitotype in our yeast species comparison. To test the
124 latter prediction, we measured carrying capacity during growth in liquid glucose medium at
125 39°C, for each of our cybrid strains harboring *S. cerevisiae* mitochondrial DNA in Z1 *S.*
126 *paradoxus*. Results revealed a 10% to 70% improvement in accumulated biomass in this assay,
127 relative to wild-type *S. paradoxus,* in all cybrids except the one for which *S. cerevisiae* Y55 was
128 the mitochondrial donor (Figure 2A). Thus, *S. cerevisiae* mitotypes were sufficient to confer
129 thermotolerance benefits, in some cases sizeable ones, in *S. paradoxus*. Interestingly, after 24
130 hours of incubation at 39°C, only *S. cerevisiae* wild-type cells retained viability, whereas cultures
131 of all strains in the *S. paradoxus* background harbored very few viable cells (Figure S3). We
132 conclude that in our cybrids, *S. cerevisiae* mitochondrial DNAs enable additional cell divisions
133 during high-temperature exposure, though failures of factors encoded by the *S. paradoxus*
134 nuclear genome ultimately prevent further growth and kill cells outright.

135 Thermotolerance phenotypes as they varied across our panel of strains correlated tightly with
136 the respiratory behaviors we had documented in assays of growth in non-fermentable carbon
137 sources (Figures 2A and 2B) and MTT reduction (Figure 3). That is, among our strains, those
138 performing best in respiratory contexts were the most thermotolerant, and the worst in
139 respiratory assays grew the worst at high temperature. These results are most consistent with a
140 causal relationship between the traits, whereby the *S. cerevisiae* mitotypes that foster better
141 thermotolerance do it by improving respiration—a metabolic underpinning for the capacity to
142 grow under high-temperature challenge.

143 **Antagonistic pleiotropy by _S. cerevisiae_ mitotypes in temperate conditions and ethanol**

144 Previous studies using interspecies hybrids have reported a defect in cold temperatures
145 attributable to *S. cerevisiae* mitotypes relative to those of *S. paradoxus* or other relatives (Baker
146 et al. 2019; Li et al. 2019; Hewitt et al. 2020). To test whether such effects would be
147 recapitulated in purebred backgrounds, for each of our Z1 *S. paradoxus* derivatives carrying *S.*
148 *cerevisiae* mitochondrial DNA, we assayed the carrying capacity after culture 23°C in liquid
149 glucose medium, for comparison against a 28°C control and the high-temperature condition
150 (39°C), also with glucose as a carbon source. The results revealed compromised carrying

151 capacity at 23°C in the cybrids that performed the best at high temperature (Figure 2A). This set
152 up an almost perfect anticorrelation between 23°C growth and thermotolerance across strains
153 (Figure 2C), mirroring the observation we had made with respiratory behaviors (Figures 2 and
154 3). We conclude that *S. cerevisiae* mitotypes have specialized to heat stress at the expense of
155 performance at lower temperatures, suggestive of fine-tuning by evolution of the temperature
156 optima of respiratory reactions encoded by the mitochondrial genome.

157 We also noted an anticorrelation across our cybrids between thermotolerance and carrying
158 capacity in glucose at 28°C: at the latter temperature, the most thermotolerant strains harboring
159 *S. cerevisiae* DNA performed the worst (Figure 2A). To explore potential drivers of this pattern,
160 we also assayed carrying capacity at 28°C in medium with ethanol as the carbon source, in
161 which we observed most cybrids carrying *S. cerevisiae* mitochondrial DNA to be at a
162 disadvantage (Figure 2A). Growth patterns among strains at 28°C and in ethanol were robustly
163 correlated (Figure 2D), suggestive of a mechanistic relationship between them, as expected
164 given that *Saccharomyces* species catabolize ethanol late in the growth cycle after having
165 secreted it (Piskur et al. 2006). In summary, based on our growth and respiration profiles, we
166 conclude that *S. cerevisiae* mitochondrial genomes are drivers of a phenotypic syndrome that
167 includes advantages in most facets of respiration as well as high-temperature growth, and
168 disadvantages at cooler temperatures and during ethanol utilization.

169 **Positive epistasis between mitochondria and nuclear genomes in terms of**
170 **thermotolerance**

171 During the evolution of *S. cerevisiae* as a species, the pro-thermotolerance mitotypes we study
172 here would have arisen alongside changes in nuclear genes which could modify their effects.
173 We sought to shed light on these relationships by modeling them in the *S. paradoxus*
174 background. To this end, we introduced *S. cerevisiae* mitochondrial genomes into a derivative of
175 *S. paradoxus* Z1 that also harbored the alleles from the DBVPG1373 Dutch soil strain of *S.*
176 *cerevisiae* at eight nuclear loci which contribute to thermotolerance (*AFG2, APC1, CEP3, DYN1,*
177 *ESP1, MYO1, SCC2*, and *TAF2*, most of which encode cell division factors; (AlZaben et al.
178 2021)). In assays of carrying capacity at 39°C, the combination of *S. cerevisiae* alleles in the
179 nuclear and mitochondrial genomes together conferred a two-fold improvement relative to wild-
180 type *S. paradoxus* (Figure 4, squares); this represented an increase in cell divisions early in the
181 treatment, as no cybrids harboring *S. cerevisiae* nuclear alleles maintained viability after 24
182 hours at 39°C (Figure S5), paralleling results from cybrids in the wild-type *S. paradoxus* nuclear
183 background (Figure S3). Advantages in carrying capacity at 39°C manifested regardless of the
184 origin of the mitotype: mitochondrial DNA from each of the four *S. cerevisiae* strain donors
185 yielded identical high-temperature growth in *S. paradoxus* in the presence of the nuclear
186 thermotolerance genes from *S. cerevisiae,* including the Y55 mitotype that had compromised
187 the phenotype in wild-type *S. paradoxus* (Figures 2A and 4). Thus, the latter incompatibility was
188 resolved by *S. cerevisiae* alleles at our focal nuclear genes.

189 Also evident from our nuclear-mitochondrial transgenic strain panel was a pattern of positive
190 epistasis. That is, the impact of each *S. cerevisiae* mitotype on thermotolerance was greater in
191 the *S. paradoxus* derivative also harboring nuclear alleles from *S. cerevisiae* than in otherwise
192 wild-type *S. paradoxus* (Figure 4; compare circles and squares). Thus, mitochondrial DNA from
193 distinct *S. cerevisiae* donors, including Y55, all achieved peak performance at high temperature
194 in the presence of *S. cerevisiae* nuclear genes; no such dependence was detectable in 28°C
195 cultures (Figure S4). Interestingly, the *S. cerevisiae* mitotype that promoted thermotolerance
196 most strongly on its own in the *S. paradoxus* background, from DBVPG1373, benefited the least
197 from the addition of DBVPG1373 alleles of nuclear genes (Figure 4, magenta). Relative to this
198 transgenic, strains harboring other *S. cerevisiae* mitotypes, which had less impact on their own,

199 achieved the same carrying capacity at 39°C in the presence of DBVPG1373 nuclear alleles
200 (Figure 4, blue, green, and orange). These results are most consistent with a ceiling beyond
201 which any *S. cerevisiae* alleles of the mitochondrial genome, even when combined with *S.*
202 *cerevisiae* alleles of our eight focal nuclear genes, are unable to improve thermotolerance, in
203 the face of defects accruing from other *S. paradoxus* loci. Nonetheless, our data make clear that
204 pro-thermotolerance alleles of mitochondrial DNAs and nuclear genes from *S. cerevisiae*
205 together contribute to the phenotype in a manner that exceeds the sum of their parts.

206 Discussion

207 A key goal of comparative genetics is to understand how evolution builds traits over long
208 timescales. In this work, we have leveraged tractable *Saccharomyces* as a testbed for the study
209 of interspecies trait genetics and evolution focused on the mitochondrial genome. Given the
210 evidence that *S. cerevisiae* thermotolerance is the product of positive selection (Weiss et al.
211 2018; Abrams et al. 2021), it serves as a useful model of the evolutionary genetics of adaptation
212 over deep divergences. Our findings complement previous studies of mitotype effects in this
213 system (Baker et al. 2019; Li et al. 2019; Hewitt et al. 2020) by tracing the phenotypes conferred
214 by *S. cerevisiae* mitochondrial alleles in purebred backgrounds, including their genetic
215 dependencies.

216 Our results shed new light on the genetic architecture and evolution of thermotolerance. Our
217 finding of a 70% boost in the trait by an *S. cerevisiae* mitotype outstrips the effect of any one of
218 the nuclear loci previously reported in this system (Weiss et al. 2018). That said, not all *S.*
219 *cerevisiae* mitotypes had a benefit of this magnitude, as might be expected given the extensive
220 precedent for polymorphism among mitochondrial genomes and their effects on human disease
221 (Wallace 2015) as well as traits in animals (Tsai and St. John 2016; Brand et al. 2024; Serrano
222 et al. 2024) and plants (Dubrovina and Kiselev 2016; Adhikari et al. 2019; Jo et al. 2019). Some
223 of the *S. cerevisiae* mitotypes we study here could be ancient, if each was part of a soft
224 selective sweep in the ancestral population when the trait arose, of the kind reported recently in
225 a plant selfing system (Bergero et al. 2019). Perhaps more plausibly, *S. cerevisiae* mitochondrial
226 polymorphisms could be the product of recent mutations on a background that underwent a
227 hard sweep long ago.

228 Our data also make clear that alongside largely beneficial marginal effects, all *S. cerevisiae*
229 mitotypes are even more advantageous at high temperature in the context of pro-
230 thermotolerance nuclear alleles. To date, such evidence for positive epistasis has been at a
231 premium in the literature describing adaptive loci from the wild (Nelson and Grishin 2018;
232 Syenina et al. 2020; Stern et al. 2022). This may be in part owing to a heavier emphasis in the
233 field on the evolutionarily difficult repacking of a given protein interior to achieve fitness
234 (Weinreich et al. 2005; Starr and Thornton 2016), which could be more constrained than
235 combinations of adaptive alleles of multiple proteins. But even the unlinked nuclear genes
236 underlying S*. cerevisiae* thermotolerance do not exhibit positive epistasis among themselves
237 (though their combinations do boost the trait; AlZaben et al. 2021). As such, our data point to
238 mitoalleles, during the evolution of *S. cerevisiae* thermotolerance, as candidate cases of
239 especially easily accessible (Liao et al. 2022) and highly beneficial mutations collected by the
240 ancestral population on the trajectory toward its final phenotype, the so-called low-hanging fruit
241 (Lenski 2017) of the adaptive process.

242 Though our data leave open the precise mechanism for these benefits, we propose that *S.*
243 *cerevisiae* mitotypes produce extra energy and metabolites (Malecki et al. 2020) during thermal
244 stress via enhanced respiration, relative to the putative ancestral behaviors of mitochondria from
245 *S. paradoxus*. If so, an excess of basic building blocks would support the capacity of *S.*

246 *cerevisiae* nuclear genes to confer their effects—those we study here govern housekeeping
247 functions, namely cell division and transcription/translation. Indeed, evidence for epistasis
248 between mitochondrial and nuclear genomes is rife in non-adaptive contexts, including
249 reproductive barriers and aging and disease (Ellison and Burton 2008; Arnqvist et al. 2010;
250 Tranah 2011; Joseph et al. 2013; Lovell et al. 2015; Roux et al. 2016; Loewen and Ganetzky
251 2018; Wolters et al. 2018; Sujkowski et al. 2019; Nguyen et al. 2020; Bushel et al. 2022; Biot-
252 Pelletier et al. 2023; Nguyen et al. 2023; Ibrahim et al. 2024 Sep 3). For *S. cerevisiae*
253 thermotolerance, the emerging model from our work and that of others is that evolution can use
254 mitonuclear interactions for gains of function, as traits are built from variants in both genome
255 compartments.

256 Likewise, the growth defects we have seen by cybrids at lower temperatures dovetail with
257 results from studies of *S. cerevisiae* nuclear thermotolerance loci and those using interspecies
258 backgrounds (Baker et al. 2019; Li et al. 2019; Hewitt et al. 2020; AlZaben et al. 2021). As a
259 general rule, evolutionary tradeoffs are routine in the adaptation literature, from prokaryotes
260 (Abram et al. 2021; Backman et al. 2024; Dalldorf et al. 2024) to animals (Ou et al. 2020;
261 Ackermans 2023; Metzler et al. 2023) and plants (Gao et al. 2022; He et al. 2022; Kurepa and
262 Smalle 2023). For yeast in particular, the exact mechanism of antagonistic pleiotropy exhibited
263 by thermotolerance loci in cooler conditions remains unclear. Exciting recent work has revealed
264 that *S. cerevisiae* proteins, including those encoded by mitochondria, are more thermostable
265 than those of sister species, establishing the likely biochemical underpinning of the trait
266 (Walunjkar et al. 2024). But it may not follow that the *S. cerevisiae* alleles of the loci we study
267 here compromise protein structure *per se* at low temperatures (Yang et al. 2015; Cui et al.
268 2024). Amino acid changes unique to *S. cerevisiae* could well have tuned the temperature
269 optima of many enzymes, as appears to be the case for the thermotolerance gene *DYN1* (Hong
270 et al. 2016). Further work will be required to pinpoint exactly what biochemical functionality *S.*
271 *cerevisiae* gave up as it acquired pro-thermotolerance alleles. As they stand, however, the
272 genetics of this system help tell a story of a complex balancing act by evolution along the *S.*
273 *cerevisiae* lineage, as nuclear and mitochondrial variants worked together to convert a
274 thermosensitive ancestor to a high-temperature specialist.

275 Acknowledgements

276 The authors thank members of the Brem lab for experimental support and helpful
277 discussions. This work was supported by NIH 2R01GM120430 to R.B.B.

278 Materials and methods

279 Strain construction

280 Strains used in this study are listed in Table S1. For phenotyping in Figure S1, we used wild-
281 type, homozygous diploid *S. cerevisiae*, DBVPG1373, YPS128, DBVPG6044 and Y55, and *S.*
282 *paradoxus* strains, Z1, UFRJ50816, A4 and KPN3828, from the Saccharomyces Genome
283 Resequencing Project (SGRP) collection (Table S1) (Cubillos et al. 2009). To make haploid
284 strains for the recipients for *S. cerevisiae* mitochondrial DNA, we first generated prototrophic
285 versions of diploid *S. paradoxus* Z1 and the *S. paradoxus* harboring the 8 *S. cerevisiae* loci,
286 designated as 8X (AlZaben et al. 2021). For this, the *HO* loci of the diploid wild-type Z1 and 8X
287 strains were knocked out using the hygromycin resistance gene as the selection marker using
288 the transformation protocol from (Reuß et al. 2004), with selection on 200 μg/ml hygromycin and
289 PCR and sequence confirmation. The resulting *ho*Δ::Hyg diploid strains were induced to
290 sporulate essentially as in (Lee et al. 2008), and mating types of the resulting haploids were
291 checked via halo assay following the protocol in (Hoffman et al. 2002), using JRY02375 and

292 JRY02176 as the mating testers. Next, for haploid MATα *S. paradoxus* Z1 and its descendant
293 8X, we generated a petite version of each (lacking mitochondrial DNA, ρ^0), using the protocol
294 adopted from (Amine et al. 2021).

295 Finally, we used wild-type, MATα haploid, G418-resistant, hygromycin-resistant *S. cerevisiae*
296 strains (DBVPG1373, YPS128, DBVPG6044 and Y55) mitochondrial DNA from the SGRP
297 collection (Table S1) (Cubillos et al. 2009) as donors of mitochondrial DNA for cybrids in our *S.*
298 *paradoxus* wild-type and 8X backgrounds. Our method for cybrid construction used the
299 cytoduction protocol of (Nguyen et al. 2020) as follows. We first constructed a heterokaryon-
300 competent *S. cerevisiae* strain harboring each mitotype of interest, referred to as a carrier. For
301 this, a single colony of each donor in turn, and a single colony of the ρ^0 *kar1*-d15 mutant
302 (JRY5450, a generous gift from Dr. Jasper Rine), were each inoculated into a separate 3 mL of
303 liquid YPD (1% yeast extract, 2% peptone, 2% glucose) and incubated at 28°C overnight with
304 shaking at 250 rpm. We mixed 100 μL of the two, spotted on a YPD plate, and incubated at
305 28°C for 4 hours. The mixed cellular patch was inoculated into 3 mL of YPD and incubated at
306 28°C for 2 hours with shaking at 250 rpm to promote cell division. After a 2-hour incubation, 10^{-5}
307 OD_{600} of cells were spread on a YPG plate (1% yeast extract, 2% peptone, 2% glycerol) to
308 select for mitochondrial genome retention. Colonies on the YPG plates were transferred to a
309 YPD plate with 200 μg/mL hygromycin or 200 μg/mL G418 to check for hygromycin and G418
310 sensitivity; we earmarked and preserved drug-sensitive, respiration-competent strains as those
311 in which the donor mitochondrial DNA had successfully been transferred to the JRY5450
312 nuclear background. We next used each carrier strain in turn to transfer the *S. cerevisiae*
313 mitochondrial DNA of interest into the haploid *S. paradoxus* Z1 ρ^0 strain and, separately, its
314 descendant, the 8X ρ^0 strain. This cytoduction proceeded as above except that the carrier and
315 the *S. paradoxus* strain were mated and the progeny were selected on YPG alone; afterward we
316 subjected them to the halo assay, to eliminate the carrier-*S. paradoxus* diploid hybrids, and only
317 those strains that behaved as haploid MATα were retained as cybrids.

318 **Growth assays**

319 Measurements of carrying capacity at 39°C were done as described (AlZaben et al. 2021) with
320 some modifications. To make sure the cells were respiratory-competent before the assay,
321 strains were streaked on YPG plates and were allowed to grow at 28°C for 4 days to form
322 colonies. Three colonies were inoculated into 15 mL of liquid YPG and incubated at 28°C for
323 overnight with shaking at 250 rpm. The cultures would reach 0.4-0.8 OD_{600} after a 16-hour
324 growth. The cultures were then back-diluted into 5 mL of YPD, YPE (1% yeast extract, 2%
325 peptone, 2% ethanol), or YPG to achieve 0.1 OD_{600}/mL, and then incubated at 23°C, 28°C or
326 39°C for 24 hours. This procedure, from streaking on solid agar plates to biomass
327 measurement, was repeated at least twice for each strain with three technical repeats in each
328 biological replicate. We collected the readouts of carrying capacity from all the replicates across
329 all days for a given strain and compared each mitochondrial transgenic to *S. paradoxus* with a
330 two-tailed Mann-Whitney U test. For epistatic analysis, a two-way ANOVA test was carried out to
331 examine the impact of the genotype-mitotype interaction on thermotolerance. All the statistical
332 analyses were done with scipy.stats in Python 3.7.

333 **MTT assay**

334 To measure respiration efficiency, pre-culture and treatment were as in Growth assays, above,
335 and after 24 hours we carried out the MTT assay as in (Sánchez and Königsberg 2006).
336 Independent experiments from growth to MTT measurement were performed at least six times.
337 The readouts were normalized to that of wild-type *S. paradoxus* at either 28°C or 39°C. Two-

338 tailed one-sample Wilcoxon test was performed using the normalized data with a hypothesized
339 value of 1 with scipy.stats in Python 3.7.

340 **Growths of *S. cerevisiae* and *S. paradoxus* in glycerol**

341 Data are from (Liti et al. 2009) and Mann-Whitney U test was performed to compare the growths
342 of the two species in glycerol with scipy.stats in Python 3.7.

343

344 # Figure captions

345 **Figure 1. Experimental design and isolates for genetic dissection of *Saccharomyces***
346 **species variation in thermotolerance.** Top, wild-type *S. paradoxus* (left) is used as the
347 background for a cybrid (right) harboring the endogenous nuclear genome (N) and the
348 mitochondrial genome from a *S. cerevisiae* donor (orange). Bottom, strains used in this work:
349 Sp, *S. paradoxus* Z1; Sc1 to Sc4, *S. cerevisiae* DBVPG1373, YPS128, DBVPG6044 and Y55,
350 respectively.

351 **Figure 2. Condition-dependent growth and tradeoffs across *Saccharomyces* species and**
352 **cybrids. (A)** In the main plot, each cell reports cell density, as a mean across replicates ($n \geq 3$),
353 after 24 hours of growth in liquid culture in the respective condition, with glucose as the carbon
354 source unless otherwise indicated. Each column reports results from wild-type *S. paradoxus*
355 (Sp) or an isogenic cybrid harboring the mitochondrial genome from a *S. cerevisiae* donor
356 (Scmt) labeled as in Figure 1. Colors report row-normalized z-score. In the inset, data are as in
357 the main figure with the addition of wild-type *S. cerevisiae* DBVPG1373 (Sc). **(B-D)** Shown are
358 reanalyses of cell density measurements across strains from the cultures and conditions in **(A)**,
359 with respective Spearman coefficients of -0.8, 1, and 0.67. In a given panel, each dot reports
360 median across replicates ($n \geq 3$), and error bars report standard deviation. Strain labels are as
361 in **(A)**. Growth of each strain was significantly different from that of *S. paradoxus* in each
362 condition (except for *S. cerevisiae* and Sp + Scmt4 at 23°C; Sp+Scmt2, Sp+Scmt3, and Sp
363 +Scmt4 in ethanol; Sp+Scmt 4 in glycerol); two-tailed Mann-Whitney $p < 0.05$. Raw cell density
364 measurements, Spearman correlation coefficients, and statistical analyses are reported in Table
365 S2.

366 **Figure 3. *S. cerevisiae* mitotypes boost respiration in the *S. paradoxus* nuclear**
367 **background at 39°C.** In each panel, in the main plot, the *y*-axis reports measurements of the
368 reduction of 1-(4,5-dimethylthiazol-2-yl)-3,5-diphenyltetrazolium bromide after 24 hours of
369 growth of a given strain in liquid culture with glucose as the carbon source at one temperature,
370 normalized to the respective measurement wild-type *S. paradoxus*. In a given column, each
371 point reports results from one biological replicate and the bar height reports the average. The *x*-
372 axis denotes strains: wild-type *S. paradoxus* (Sp) or cybrids the mitochondrial genome from a *S.*
373 *cerevisiae* donor (Scmt) labeled as in Figure 1. In the inset, data are as in the main figure with
374 the addition of wild-type *S. cerevisiae* DBVPG1373 (Sc). **(A),** 28°C; **(B)**, 39°C. *, one-sample
375 Wilcoxon $p < 0.05$; otherwise, not significant. Raw data and statistical analyses are reported in
376 Table S2.

377 **Figure 4. Epistasis between nuclear and mitochondrial *Saccharomyces* species variants**
378 **that impact thermotolerance.** Each panel reports results from wild-type *S. paradoxus* Z1 (Sp)
379 and isogenic derivatives the mitochondrial genome from a *S. cerevisiae* donor (Scmt) labeled as
380 in Figure 1; eight nuclear thermotolerance genes from *S. cerevisiae* DBVPG1373 (8X); or both.
381 The *y*-axis reports cell density after 24 hours of growth in liquid culture at 39°C, with glucose as
382 the carbon source. In a given column, transparent points report replicates ($n \geq 6$) and the bold
383 bordered point reports their average. *, two-way ANOVA $p < 0.01$ for mito-nuclear interaction;
384 otherwise, not significant. Raw cell density measurements and statistical analyses are reported
385 in Table S2.

386

387

388

389 ## Supplementary figure captions

390 **Figure S1. Stark growth differences between *S. cerevisiae* and *S. paradoxus* at high**
391 **temperature.** In a given panel, the *y*-axis reports cell density after 24 hours of growth in liquid
392 culture of a wild-type homozygous diploid *Saccharomyces* strain in one temperature condition,
393 with glucose as the carbon source. Points reports technical replicates (n = 3) and bar heights
394 report means. Sc1, Sc2, Sc3 and Sc4 denote *S. cerevisiae* DBVPG1373, YPS128, DBVPG6044
395 and Y55, respectively. Sp1, Sp2, Sp3 and Sp4 denote *S. paradoxus* KPN3828, UFRJ50816, A4
396 and Z1, respectively. **(A)** 28°C; **(B)** 39°C. *, two-tailed Mann-Whitney $p < 0.05$; otherwise, not
397 significant. Raw cell density measurements and statistical analyses are reported in Table S2.

398 **Figure S2. Wild-type strain and species variation in growth on glycerol.** In a given panel,
399 each bar reports results from one wild-type *S. cerevisiae* or *S. paradoxus* strain grown in liquid
400 culture with glucose as the carbon source from (Warringer et al. 2011). The *y*-axis reports
401 relative growth rate **(A)** and efficiency **(B)**. *, two-talied Mann-Whitney $p < 0.05$.

402 **Figure S3. Chronic 39°C treatment is lethal to *S. paradoxus* and to its cybrids.** Shown are
403 results of plating of the indicated strains after 24 hours of culture in one temperature condition,
404 with glucose as the carbon source, followed by incubation of plates at 28°C for two days. Strains
405 were wild-type *S. cerevisiae* (Sc), wild-type *S. paradoxus* (Sp), or a cybrid in the *S. paradoxus*
406 background harboring the mitochondrial genome from a *S. cerevisiae* donor (Scmt) labeled as
407 in Figure 1 of the main text. Raw cell density measurements and statistical analyses are
408 reported in Table S2.

409 **Figure S4. No detectable epistasis between nuclear and mitochondrial *Saccharomyces***
410 **species variants that impact 28°C growth.** Labels are as in Figure 4. The *y*-axis reports cell
411 density after 24 hours of growth in liquid culture at 28°C, with glucose as the carbon source. In a
412 given column, transparent points report replicates ($n \geq 6$) and the bold bordered point reports
413 their average. ns, two-way ANOVA $p > 0.05$ for mito-nuclear interaction. Raw cell density
414 measurements and statistical analyses are reported in Table S2.

415 **Figure S5. Chronic 39°C treatment is lethal to *S. paradoxus* harboring *S. cerevisiae***
416 **nuclear thermotolerance loci and to its cybrids.** Labels are as in **Figure S3** except that the
417 strains were wild-type *S. cerevisiae* (Sc), wild-type *S. paradoxus* (Sp), *S. paradoxus* harboring
418 eight nuclear loci from *S. cerevisiae* (8X), or a cybrid in the 8X background harboring the
419 mitochondrial genome from a *S. cerevisiae* donor (Scmt) labeled as in Figure 1 of the main text.
420 Raw cell density measurements and statistical analyses are reported in Table S2.

421

422 ## Supplementary table captions

423 **Table S1. Strains used in this work.**

424 **Table S2. Growth data and statistics.** D1373, YPS128, D6044 and Y55 indicate *S. cerevisiae*
425 strains DBVPG1373, YPS128, DBVPG6044 and Y55, respectively; Sp, *S. paradoxus* Z1. The
426 first sheet contains all OD_{600} measurements of each strain at 39°C in standard glucose medium.
427 The second sheet reports the statistical analysis of the OD_{600} measurements of the cybrids at
428 39°C compared to wild-type *S. paradoxus* or the *S. paradoxus* harboring *S. cerevisiae* nuclear
429 loci (8X) by Mann-Whitney U test. The third sheet contains all OD_{600} measurements of each
430 strain at 28°C in standard glucose medium. The fourth sheet contains all OD_{600} measurements
431 of each strain at 28°C in medium with glycerol as a carbon source. The fifth sheet contains all
432 OD_{600} measurements of each strain at 28°C in medium with ethanol as a carbon source. The
433 sixth sheet contains all OD_{600} measurements of each strain at 23°C in standard glucose
434 medium. The seventh sheet reports the *p*-values of two-way ANOVA of the impact of the
435 interaction between *S. cerevisiae* mitotypes and the 8 *S. cerevisiae* loci in the *S. paradoxus*
436 background on high temperature growth (Figure 4). The eighth sheet reports the raw readouts
437 of the MTT assay at 28°C and 39°C. The ninth sheet reports the *p*-values of the normalized
438 MTT measurements by one-sample Wilcoxon with a hypothesized value of 1. The tenth sheet
439 reports the Spearman correlation coefficients and respective *p*-values of Figures 2B, 2C and
440 2D. The eleventh sheet reports the OD_{600} measurements of wild-type *S. cerevisiae* and *S.*
441 *paradoxus* strains at 28°C and 39°C in standard glucose medium with the statistical analysis
442 (Figure S1). The twelfth sheet reports the *p*-values of glycerol growth efficiency and rate of the
443 wild-type *S. cerevisiae* and *S. paradoxus* strains by two-tailed Mann-Whitney U test (Warringer
444 et al. 2011).

445

446

References

Abram F, Arcari T, Guerreiro D, O'Byrne CP. 2021. Evolutionary trade-offs between growth and survival: The delicate balance between reproductive success and longevity in bacteria. In: Advances in Microbial Physiology. Vol. 79. Elsevier. p. 133–162. [accessed 2024 Dec 24]. https://linkinghub.elsevier.com/retrieve/pii/S006529112100014X.

Abrams MB, Dubin CA, AlZaben F, Bravo J, Joubert PM, Weiss CV, Brem RB. 2021. Population and comparative genetics of thermotolerance divergence between yeast species. Gresham D, editor. G3. 11(7):jkab139. doi:10.1093/g3journal/jkab139.

Ackermans NL. 2023. Neurobiological tradeoffs of headbutting bovids. Trends in Neurosciences. 46(11):898–900. doi:10.1016/j.tins.2023.08.004.

Adhikari B, Caruso CM, Case AL. 2019. Beyond balancing selection: frequent mitochondrial recombination contributes to high-female frequencies in gynodioecious *Lobelia siphilitica* (Campanulaceae). New Phytologist. 224(3):1381–1393. doi:10.1111/nph.16136.

Allen Orr H. 2001. The genetics of species differences. Trends in Ecology & Evolution. 16(7):343–350. doi:10.1016/S0169-5347(01)02167-X.

AlZaben F, Chuong JN, Abrams MB, Brem RB. 2021. Joint effects of genes underlying a temperature specialization tradeoff in yeast. Fay JC, editor. PLoS Genet. 17(9):e1009793. doi:10.1371/journal.pgen.1009793.

Amine AAA, Liao C-W, Hsu P-C, Opoc FJG, Leu J-Y. 2021. Experimental evolution improves mitochondrial genome quality control in Saccharomyces cerevisiae and extends its replicative lifespan. Current Biology. 31(16):3663-3670.e4. doi:10.1016/j.cub.2021.06.026.

Arnqvist G, Dowling DK, Eady P, Gay L, Tregenza T, Tuda M, Hosken DJ. 2010. GENETIC ARCHITECTURE OF METABOLIC RATE: ENVIRONMENT SPECIFIC EPISTASIS BETWEEN MITOCHONDRIAL AND NUCLEAR GENES IN AN INSECT: GENETIC ARCHITECTURE OF METABOLIC RATE. Evolution. 64(12):3354–3363. doi:10.1111/j.1558-5646.2010.01135.x.

Backman T, Burbano HA, Karasov TL. 2024. Tradeoffs and constraints on the evolution of tailocins. Trends in Microbiology. 32(11):1084–1095. doi:10.1016/j.tim.2024.04.001.

Baker EP, Peris D, Moriarty RV, Li XC, Fay JC, Hittinger CT. 2019. Mitochondrial DNA and temperature tolerance in lager yeasts. Sci Adv. 5(1):eaav1869. doi:10.1126/sciadv.aav1869.

Bazzicalupo A. 2022. Local adaptation in fungi. FEMS Microbiology Reviews. 46(6):fuac026. doi:10.1093/femsre/fuac026.

Bergero R, Levsen N, Wolff K, Charlesworth D. 2019. Data from: Arms races with mitochondrial genome soft sweeps in a gynodioecious plant, Plantago lanceolata. :78254

bytes. doi:10.5061/DRYAD.TH757VG. [accessed 2025 Mar 4]. https://datadryad.org/dataset/doi:10.5061/dryad.th757vg.

Biot-Pelletier D, Bettinazzi S, Gagnon-Arsenault I, Dubé AK, Bédard C, Nguyen THM, Fiumera HL, Breton S, Landry CR. 2023. Evolutionary Trajectories are Contingent on Mitonuclear Interactions. Zhang J, editor. Molecular Biology and Evolution. 40(4):msad061. doi:10.1093/molbev/msad061.

Bozdag GO, Ono J, Denton JA, Karakoc E, Hunter N, Leu J-Y, Greig D. 2021. Breaking a species barrier by enabling hybrid recombination. Current Biology. 31(4):R180–R181. doi:10.1016/j.cub.2020.12.038.

Brand JA, Garcia-Gonzalez F, Dowling DK, Wong BBM. 2024. Mitochondrial genetic variation as a potential mediator of intraspecific behavioural diversity. Trends in Ecology & Evolution. 39(2):199–212. doi:10.1016/j.tree.2023.09.009.

Bushel PR, Ward J, Burkholder A, Li J, Anchang B. 2022. Mitochondrial-nuclear epistasis underlying phenotypic variation in breast cancer pathology. Sci Rep. 12(1):1393. doi:10.1038/s41598-022-05148-4.

Cao Y, Vergnes L, Wang Y-C, Pan C, Chella Krishnan K, Moore TM, Rosa-Garrido M, Kimball TH, Zhou Z, Charugundla S, et al. 2022. Sex differences in heart mitochondria regulate diastolic dysfunction. Nat Commun. 13(1):3850. doi:10.1038/s41467-022-31544-5.

Chou J-Y, Hung Y-S, Lin K-H, Lee H-Y, Leu J-Y. 2010. Multiple Molecular Mechanisms Cause Reproductive Isolation between Three Yeast Species. Noor MAF, editor. PLoS Biol. 8(7):e1000432. doi:10.1371/journal.pbio.1000432.

Chou J-Y, Leu J-Y. 2015. The Red Queen in mitochondria: cyto-nuclear co-evolution, hybrid breakdown and human disease. Front Genet. 6. doi:10.3389/fgene.2015.00187. [accessed 2025 Feb 18]. http://www.frontiersin.org/Evolutionary_and_Population_Genetics/10.3389/fgene.2015.00187/abstract.

Crandall JG, Fisher KJ, Sato TK, Hittinger CT. 2023. Ploidy evolution in a wild yeast is linked to an interaction between cell type and metabolism. Zanders SE, editor. PLoS Biol. 21(11):e3001909. doi:10.1371/journal.pbio.3001909.

Cubillos FA, Louis EJ, Liti G. 2009. Generation of a large set of genetically tractable haploid and diploid *Saccharomyces* strains. FEMS Yeast Research. 9(8):1217–1225. doi:10.1111/j.1567-1364.2009.00583.x.

Cui S, Furukawa R, Akanuma S. 2024. Insights into the low-temperature adaptation of an enzyme as studied through ancestral sequence reconstruction. doi:10.1101/2024.09.05.611558. [accessed 2024 Dec 16]. http://biorxiv.org/lookup/doi/10.1101/2024.09.05.611558.

Dalldorf C, Rychel K, Szubin R, Hefner Y, Patel A, Zielinski DC, Palsson BO. 2024. The hallmarks of a tradeoff in transcriptomes that balances stress and growth functions. Fodor A, editor. mSystems. 9(7):e00305-24. doi:10.1128/msystems.00305-24.

De Chiara M, Friedrich A, Barré B, Breitenbach M, Schacherer J, Liti G. 2020. Discordant evolution of mitochondrial and nuclear yeast genomes at population level. BMC Biol. 18(1):49. doi:10.1186/s12915-020-00786-4.

Dubrovina AS, Kiselev KV. 2016. Age-associated alterations in the somatic mutation and DNA methylation levels in plants. Weber A, editor. Plant Biol J. 18(2):185–196. doi:10.1111/plb.12375.

Elena SF. 2017. Local adaptation of plant viruses: lessons from experimental evolution. Molecular Ecology. 26(7):1711–1719. doi:10.1111/mec.13836.

Ellison CK, Burton RS. 2008. Genotype-dependent variation of mitochondrial transcriptional profiles in interpopulation hybrids. Proc Natl Acad Sci USA. 105(41):15831–15836. doi:10.1073/pnas.0804253105.

Ferreira T, Rodriguez S. 2024. Mitochondrial DNA: Inherent Complexities Relevant to Genetic Analyses. Genes. 15(5):617. doi:10.3390/genes15050617.

Forejt J, Jansa P. 2023. Meiotic Recognition of Evolutionarily Diverged Homologs: Chromosomal Hybrid Sterility Revisited. Malik H, editor. Molecular Biology and Evolution. 40(4):msad083. doi:10.1093/molbev/msad083.

Fredericks LR, Lee MD, Crabtree AM, Boyer JM, Kizer EA, Taggart NT, Roslund CR, Hunter SS, Kennedy CB, Willmore CG, et al. 2021. The Species-Specific Acquisition and Diversification of a K1-like Family of Killer Toxins in Budding Yeasts of the Saccharomycotina. PLoS Genet. 17(2):e1009341. doi:10.1371/journal.pgen.1009341.

Gao H, Cui J, Liu S, Wang S, Lian Y, Bai Y, Zhu T, Wu H, Wang Y, Yang S, et al. 2022. Natural variations of ZmSRO1d modulate the trade-off between drought resistance and yield by affecting ZmRBOHC-mediated stomatal ROS production in maize. Molecular Plant. 15(10):1558–1574. doi:10.1016/j.molp.2022.08.009.

Gonçalves P, Valério E, Correia C, De Almeida JMGCF, Sampaio JP. 2011. Evidence for Divergent Evolution of Growth Temperature Preference in Sympatric Saccharomyces Species. Chaturvedi V, editor. PLoS ONE. 6(6):e20739. doi:10.1371/journal.pone.0020739.

He Z, Webster S, He SY. 2022. Growth–defense trade-offs in plants. Current Biology. 32(12):R634–R639. doi:10.1016/j.cub.2022.04.070.

Hénault M, Marsit S, Charron G, Landry CR. 2022. Hybridization drives mitochondrial DNA degeneration and metabolic shift in a species with biparental mitochondrial inheritance. Genome Res. 32(11–12):2043–2056. doi:10.1101/gr.276885.122.

Hewitt SK, Duangrattanalert K, Burgis T, Zeef LAH, Naseeb S, Delneri D. 2020. Plasticity of Mitochondrial DNA Inheritance and its Impact on Nuclear Gene Transcription in Yeast Hybrids. Microorganisms. 8(4):494. doi:10.3390/microorganisms8040494.

Hoffman GA, Garrison TR, Dohlman HG. 2002. Analysis of RGS Proteins in Saccharomyces cerevisiae. In: Methods in Enzymology. Vol. 344. Elsevier. p. 617–631. [accessed 2024 Dec 17]. https://linkinghub.elsevier.com/retrieve/pii/S0076687902447441.

Hong W, Takshak A, Osunbayo O, Kunwar A, Vershinin M. 2016. The Effect of Temperature on Microtubule-Based Transport by Cytoplasmic Dynein and Kinesin-1 Motors. Biophysical Journal. 111(6):1287–1294. doi:10.1016/j.bpj.2016.08.006.

Hou J, Friedrich A, de Montigny J, Schacherer J. 2014. Chromosomal Rearrangements as a Major Mechanism in the Onset of Reproductive Isolation in Saccharomyces cerevisiae. Current Biology. 24(10):1153–1159. doi:10.1016/j.cub.2014.03.063.

Houtkooper RH, Mouchiroud L, Ryu D, Moullan N, Katsyuba E, Knott G, Williams RW, Auwerx J. 2013. Mitonuclear protein imbalance as a conserved longevity mechanism. Nature. 497(7450):451–457. doi:10.1038/nature12188.

Ibrahim R, Bahilo Martinez M, Dobson AJ. 2024 Sep 3. Rapamycin's lifespan effect is modulated by mito-nuclear epistasis in *Drosophila*. Aging Cell.:e14328. doi:10.1111/acel.14328.

Jain AK, Singh D, Dubey K, Maurya R, Mittal S, Pandey AK. 2018. Models and Methods for In Vitro Toxicity. In: In Vitro Toxicology. Elsevier. p. 45–65. [accessed 2025 Feb 25]. https://linkinghub.elsevier.com/retrieve/pii/B9780128046678000031.

Jhuang H, Lee H, Leu J. 2017. Mitochondrial–nuclear co-evolution leads to hybrid incompatibility through pentatricopeptide repeat proteins. EMBO Reports. 18(1):87–101. doi:10.15252/embr.201643311.

Jo YD, Lee H-Y, Ro N-Y, Kim SH, Kim J-B, Kang B-C, Kang S-Y. 2019. Mitotypes Based on Structural Variation of Mitochondrial Genomes Imply Relationships With Morphological Phenotypes and Cytoplasmic Male Sterility in Peppers. Front Plant Sci. 10:1343. doi:10.3389/fpls.2019.01343.

Joseph B, Corwin JA, Li B, Atwell S, Kliebenstein DJ. 2013. Cytoplasmic genetic variation and extensive cytonuclear interactions influence natural variation in the metabolome. eLife. 2:e00776. doi:10.7554/eLife.00776.

Kellis M, Patterson N, Endrizzi M, Birren B, Lander ES. 2003. Sequencing and comparison of yeast species to identify genes and regulatory elements. Nature. 423(6937):241–254. doi:10.1038/nature01644.

586 Kraemer SA, Boynton PJ. 2017. Evidence for microbial local adaptation in nature. Molecular
587 Ecology. 26(7):1860–1876. doi:10.1111/mec.13958.

588 Kurepa J, Smalle JA. 2023. Plant Hormone Modularity and the Survival-Reproduction Trade-
589 Off. Biology. 12(8):1143. doi:10.3390/biology12081143.

590 Leducq J-B, Henault M, Charron G, Nielly-Thibault L, Terrat Y, Fiumera HL, Shapiro BJ,
591 Landry CR. 2017. Mitochondrial Recombination and Introgression during Speciation by
592 Hybridization. Molecular Biology and Evolution. 34(8):1947–1959.
593 doi:10.1093/molbev/msx139.

594 Lee H-Y, Chou J-Y, Cheong L, Chang N-H, Yang S-Y, Leu J-Y. 2008. Incompatibility of Nuclear
595 and Mitochondrial Genomes Causes Hybrid Sterility between Two Yeast Species. Cell.
596 135(6):1065–1073. doi:10.1016/j.cell.2008.10.047.

597 Lenski RE. 2017. Experimental evolution and the dynamics of adaptation and genome
598 evolution in microbial populations. The ISME Journal. 11(10):2181–2194.
599 doi:10.1038/ismej.2017.69.

600 Li XC, Peris D, Hittinger CT, Sia EA, Fay JC. 2019. Mitochondria-encoded genes contribute to
601 evolution of heat and cold tolerance in yeast. Sci Adv. 5(1):eaav1848.
602 doi:10.1126/sciadv.aav1848.

603 Liao S, Chen L, Song Z, He H. 2022. The fate of damaged mitochondrial DNA in the cell.
604 Biochimica et Biophysica Acta (BBA) - Molecular Cell Research. 1869(5):119233.
605 doi:10.1016/j.bbamcr.2022.119233.

606 Liti G, Carter DM, Moses AM, Warringer J, Parts L, James SA, Davey RP, Roberts IN, Burt A,
607 Koufopanou V, et al. 2009. Population genomics of domestic and wild yeasts. Nature.
608 458(7236):337–341. doi:10.1038/nature07743.

609 Loewen CA, Ganetzky B. 2018. Mito-Nuclear Interactions Affecting Lifespan and
610 Neurodegeneration in a *Drosophila* Model of Leigh Syndrome. Genetics. 208(4):1535–1552.
611 doi:10.1534/genetics.118.300818.

612 Lovell JT, Mullen JL, Lowry DB, Awole K, Richards JH, Sen S, Verslues PE, Juenger TE, McKay
613 JK. 2015. Exploiting Differential Gene Expression and Epistasis to Discover Candidate
614 Genes for Drought-Associated QTLs in *Arabidopsis thaliana*. Plant Cell. 27(4):969–983.
615 doi:10.1105/tpc.15.00122.

616 Lupo O, Krieger G, Jonas F, Barkai N. 2021. Accumulation of *cis* - and *trans* -regulatory
617 variations is associated with phenotypic divergence of a complex trait between yeast
618 species. Andrews B, editor. G3 Genes|Genomes|Genetics. 11(2):jkab016.
619 doi:10.1093/g3journal/jkab016.

Malecki M, Kamrad S, Ralser M, Bähler J. 2020. Mitochondrial respiration is required to provide amino acids during fermentative proliferation of fission yeast. EMBO Reports. 21(11):e50845. doi:10.15252/embr.202050845.

Mário Š, PolÃ¡kovÃ¡ S, JatzovÃ¡ K, Sulo P. 2015. Post-zygotic sterility and cytonuclear compatibility limits in S. cerevisiae xenomitochondrial cybrids. Front Genet. 5. doi:10.3389/fgene.2014.00454. [accessed 2024 Nov 7]. http://journal.frontiersin.org/article/10.3389/fgene.2014.00454/abstract.

Marsit S, Hénault M, Charron G, Fijarczyk A, Landry CR. 2021. The neutral rate of whole-genome duplication varies among yeast species and their hybrids. Nat Commun. 12(1):3126. doi:10.1038/s41467-021-23231-8.

Melvin RG, Ballard JWO. 2006. Intraspecific variation in survival and mitochondrial oxidative phosphorylation in wild-caught *Drosophila simulans*. Aging Cell. 5(3):225–233. doi:10.1111/j.1474-9726.2006.00211.x.

Meng X, Li L, Pascual J, Rahikainen M, Yi C, Jost R, He C, Fournier-Level A, Borevitz J, Kangasjärvi S, et al. 2022. GWAS on multiple traits identifies mitochondrial ACONITASE3 as important for acclimation to submergence stress. Plant Physiology. 188(4):2039–2058. doi:10.1093/plphys/kiac011.

Metzler S, Kirchner J, Grasse AV, Cremer S. 2023. Trade-offs between immunity and competitive ability in fighting ant males. BMC Ecol Evo. 23(1):37. doi:10.1186/s12862-023-02137-7.

Moran BM, Payne CY, Powell DL, Iverson ENK, Donny AE, Banerjee SM, Langdon QK, Gunn TR, Rodriguez-Soto RA, Madero A, et al. 2024. A lethal mitonuclear incompatibility in complex I of natural hybrids. Nature. 626(7997):119–127. doi:10.1038/s41586-023-06895-8.

Nelson ED, Grishin NV. 2018. Inference of epistatic effects in a key mitochondrial protein. Phys Rev E. 97(6):062404. doi:10.1103/PhysRevE.97.062404.

Nguyen THM, Sondhi S, Ziesel A, Paliwal S, Fiumera HL. 2020. Mitochondrial-nuclear coadaptation revealed through mtDNA replacements in Saccharomyces cerevisiae. BMC Evol Biol. 20(1):128. doi:10.1186/s12862-020-01685-6.

Nguyen THM, Tinz-Burdick A, Lenhardt M, Geertz M, Ramirez F, Schwartz M, Toledano M, Bonney B, Gaebler B, Liu W, et al. 2023. Mapping mitonuclear epistasis using a novel recombinant yeast population. Hopper AK, editor. PLoS Genet. 19(3):e1010401. doi:10.1371/journal.pgen.1010401.

Nikolov LA, Tsiantis M. 2015. Interspecies Gene Transfer as a Method for Understanding the Genetic Basis for Evolutionary Change: Progress, Pitfalls, and Prospects. Front Plant Sci. 6:1135. doi:10.3389/fpls.2015.01135.

Oppong RF, Terracciano A, Picard M, Qian Y, Butler TJ, Tanaka T, Moore AZ, Simonsick EM, Opsahl-Ong K, Coletta C, et al. 2022. Personality traits are consistently associated with blood mitochondrial DNA copy number estimated from genome sequences in two genetic cohort studies. eLife. 11:e77806. doi:10.7554/eLife.77806.

Ou Q, Vannier J, Yang X, Chen A, Mai H, Shu D, Han J, Fu D, Wang R, Mayer G. 2020. Evolutionary trade-off in reproduction of Cambrian arthropods. Sci Adv. 6(18):eaaz3376. doi:10.1126/sciadv.aaz3376.

Paget CM, Schwartz J-M, Delneri D. 2014. Environmental systems biology of cold-tolerant phenotype in Saccharomyces species adapted to grow at different temperatures. Mol Ecol. 23(21):5241–5257. doi:10.1111/mec.12930.

Pakendorf B, Stoneking M. 2005. MITOCHONDRIAL DNA AND HUMAN EVOLUTION. Annu Rev Genom Hum Genet. 6(1):165–183. doi:10.1146/annurev.genom.6.080604.162249.

Parra M, Libkind D, Hittinger CT, Álvarez L, Bellora N. 2023. Assembly and comparative genome analysis of a Patagonian *Aureobasidium pullulans* isolate reveals unexpected intraspecific variation. Yeast. 40(5–6):197–213. doi:10.1002/yea.3853.

Peng L, Wang B, Ren P. 2005. Reduction of MTT by flavonoids in the absence of cells. Colloids and Surfaces B: Biointerfaces. 45(2):108–111. doi:10.1016/j.colsurfb.2005.07.014.

Peris D, Ubbelohde EJ, Kuang MC, Kominek J, Langdon QK, Adams M, Koshalek JA, Hulfachor AB, Opulente DA, Hall DJ, et al. 2023. Macroevolutionary diversity of traits and genomes in the model yeast genus Saccharomyces. Nat Commun. 14(1):690. doi:10.1038/s41467-023-36139-2.

Pinto J, Balarezo-Cisneros LN, Delneri D. 2025. Exploring adaptation routes to cold temperatures in the Saccharomyces genus. Peris D, editor. PLoS Genet. 21(2):e1011199. doi:10.1371/journal.pgen.1011199.

Piskur J, Rozpedowska E, Polakova S, Merico A, Compagno C. 2006. How did Saccharomyces evolve to become a good brewer? Trends in Genetics. 22(4):183–186. doi:10.1016/j.tig.2006.02.002.

Quéméneur J-B, Danion M, Cabon J, Collet S, Zambonino-Infante J-L, Salin K. 2022. The relationships between growth rate and mitochondrial metabolism varies over time. Sci Rep. 12(1):16066. doi:10.1038/s41598-022-20428-9.

Rees JS, Castellano S, Andrés AM. 2020. The Genomics of Human Local Adaptation. Trends in Genetics. 36(6):415–428. doi:10.1016/j.tig.2020.03.006.

Reuß O, Vik Å, Kolter R, Morschhäuser J. 2004. The SAT1 flipper, an optimized tool for gene disruption in Candida albicans. Gene. 341:119–127. doi:10.1016/j.gene.2004.06.021.

Rikhvanov EG, Varakina NN, Rusaleva TM, Rachenko EI, Kiseleva VA, Voinikov VK. 2001. [No title found]. Microbiology. 70(4):462–465. doi:10.1023/A:1010442429489.

Roop JI, Chang KC, Brem RB. 2016. Polygenic evolution of a sugar specialization trade-off in yeast. Nature. 530(7590):336–339. doi:10.1038/nature16938.

Roux F, Mary-Huard T, Barillot E, Wenes E, Botran L, Durand S, Villoutreix R, Martin-Magniette M-L, Camilleri C, Budar F. 2016. Cytonuclear interactions affect adaptive traits of the annual plant *Arabidopsis thaliana* in the field. Proc Natl Acad Sci USA. 113(13):3687–3692. doi:10.1073/pnas.1520687113.

Salvadó Z, Arroyo-López FN, Guillamón JM, Salazar G, Querol A, Barrio E. 2011. Temperature Adaptation Markedly Determines Evolution within the Genus *Saccharomyces*. Appl Environ Microbiol. 77(7):2292–2302. doi:10.1128/AEM.01861-10.

Sánchez NS, Königsberg M. 2006. Using yeast to easily determine mitochondrial functionality with 1-(4,5-dimethylthiazol-2-yl)-3,5-diphenyltetrazolium bromide (MTT) assay. Biochem Molecular Bio Educ. 34(3):209–212. doi:10.1002/bmb.2006.49403403209.

Serrano IM, Hirose M, Valentine CC, Roesner S, Schmidt E, Pratt G, Williams L, Salk J, Ibrahim S, Sudmant PH. 2024. Mitochondrial haplotype and mito-nuclear matching drive somatic mutation and selection throughout ageing. Nat Ecol Evol. 8(5):1021–1034. doi:10.1038/s41559-024-02338-3.

Shoemaker M, Cohen I, Campbell M. 2004. Reduction of MTT by aqueous herbal extracts in the absence of cells. Journal of Ethnopharmacology. 93(2–3):381–384. doi:10.1016/j.jep.2004.04.011.

Slater TF, Sawyer B, Sträuli U. 1963. Studies on succinate-tetrazolium reductase systems. Biochimica et Biophysica Acta. 77:383–393. doi:10.1016/0006-3002(63)90513-4.

Smukowski Heil C, Patterson K, Hickey AS-M, Alcantara E, Dunham MJ. 2021. Transposable Element Mobilization in Interspecific Yeast Hybrids. Vieira C, editor. Genome Biology and Evolution. 13(3):evab033. doi:10.1093/gbe/evab033.

Sork VL. 2017. Genomic Studies of Local Adaptation in Natural Plant Populations. Journal of Heredity. 109(1):3–15. doi:10.1093/jhered/esx091.

Starr TN, Thornton JW. 2016. Epistasis in protein evolution. Protein Science. 25(7):1204–1218. doi:10.1002/pro.2897.

Stern DB, Anderson NW, Diaz JA, Lee CE. 2022. Genome-wide signatures of synergistic epistasis during parallel adaptation in a Baltic Sea copepod. Nat Commun. 13(1):4024. doi:10.1038/s41467-022-31622-8.

723 Sujkowski A, Spierer AN, Rajagopalan T, Bazzell B, Safdar M, Imsirovic D, Arking R, Rand
724 DM, Wessells R. 2019. Mito-nuclear interactions modify Drosophila exercise performance.
725 Mitochondrion. 47:188–205. doi:10.1016/j.mito.2018.11.005.

726 Sullivan LB, Chandel NS. 2014. Mitochondrial reactive oxygen species and cancer. Cancer
727 Metab. 2(1):17. doi:10.1186/2049-3002-2-17.

728 Sulo P, Pirek M, Oltesova A, Marinoni G, Pikur J. 2003. The efficiency of functional
729 mitochondrial replacement in species has directional character. FEMS Yeast Research.
730 4(1):97–104. doi:10.1016/S1567-1356(03)00109-0.

731 Sun J, Duan X, Hoffmann AA, Liu Y, Garvin MR, Chen L, Hu G, Zhou J, Huang H, Xue X, et al.
732 2019. Mitochondrial variation in small brown planthoppers linked to multiple traits and
733 probably reflecting a complex evolutionary trajectory. Molecular Ecology. 28(14):3306–
734 3323. doi:10.1111/mec.15148.

735 Swamy KBS, Lee H-Y, Ladra C, Liu C-FJ, Chao J-C, Chen Y-Y, Leu J-Y. 2022. Proteotoxicity
736 caused by perturbed protein complexes underlies hybrid incompatibility in yeast. Nat
737 Commun. 13(1):4394. doi:10.1038/s41467-022-32107-4.

738 Sweeney J, Kuehne H, Sniegowski P. 2004. Sympatric natural and populations have
739 different thermal growth profiles. FEMS Yeast Research. 4(4–5):521–525.
740 doi:10.1016/S1567-1356(03)00171-5.

741 Syenina A, Vijaykrishna D, Gan ES, Tan HC, Choy MM, Siriphanitchakorn T, Cheng C,
742 Vasudevan SG, Ooi EE. 2020. Positive epistasis between viral polymerase and the 3'
743 untranslated region of its genome reveals the epidemiologic fitness of dengue virus. Proc
744 Natl Acad Sci USA. 117(20):11038–11047. doi:10.1073/pnas.1919287117.

745 Tranah GJ. 2011. Mitochondrial–nuclear epistasis: Implications for human aging and
746 longevity. Ageing Research Reviews. 10(2):238–252. doi:10.1016/j.arr.2010.06.003.

747 Tsai T, St. John JC. 2016. The role of mitochondrial DNA copy number, variants, and
748 haplotypes in farm animal developmental outcome. Domestic Animal Endocrinology.
749 56:S133–S146. doi:10.1016/j.domaniend.2016.03.005.

750 Vijayraghavan S, Kozmin SG, Strope PK, Skelly DA, Lin Z, Kennell J, Magwene PM, Dietrich
751 FS, McCusker JH. 2019. Mitochondrial Genome Variation Affects Multiple Respiration and
752 Nonrespiration Phenotypes in *Saccharomyces cerevisiae*. Genetics. 211(2):773–786.
753 doi:10.1534/genetics.118.301546.

754 Wallace DC. 2015. Mitochondrial DNA Variation in Human Radiation and Disease. Cell.
755 163(1):33–38. doi:10.1016/j.cell.2015.08.067.

756 Walunjkar N, Lai TY, Akhter N, Miller JH, Bettinger JQ, Marcus E, Phizicky EM,
757 Ghaemmaghami S, Fay JC. 2024. Pervasive divergence in protein thermostability is

mediated by both structural changes and cellular environments. doi:10.1101/2024.12.09.627561. [accessed 2024 Dec 16]. http://biorxiv.org/lookup/doi/10.1101/2024.12.09.627561.

Warringer J, Zörgö E, Cubillos FA, Zia A, Gjuvsland A, Simpson JT, Forsmark A, Durbin R, Omholt SW, Louis EJ, et al. 2011. Trait Variation in Yeast Is Defined by Population History. Kruglyak L, editor. PLoS Genet. 7(6):e1002111. doi:10.1371/journal.pgen.1002111.

Weinreich DM, Watson RA, Chao L. 2005. Perspective: Sign epistasis and genetic constraint on evolutionary trajectories. Evolution. 59(6):1165–1174.

Weiss CV, Brem RB. 2019. Dissecting Trait Variation across Species Barriers. Trends in Ecology & Evolution. 34(12):1131–1136. doi:10.1016/j.tree.2019.07.013.

Weiss CV, Roop JI, Hackley RK, Chuong JN, Grigoriev IV, Arkin AP, Skerker JM, Brem RB. 2018. Genetic dissection of interspecific differences in yeast thermotolerance. Nat Genet. 50(11):1501–1504. doi:10.1038/s41588-018-0243-4.

Wolff JN, Ladoukakis ED, Enríquez JA, Dowling DK. 2014. Mitonuclear interactions: evolutionary consequences over multiple biological scales. Philos Trans R Soc Lond B Biol Sci. 369(1646):20130443. doi:10.1098/rstb.2013.0443.

Wolters JF, Charron G, Gaspary A, Landry CR, Fiumera AC, Fiumera HL. 2018. Mitochondrial Recombination Reveals Mito–Mito Epistasis in Yeast. Genetics. 209(1):307–319. doi:10.1534/genetics.117.300660.

Wolters JF, Chiu K, Fiumera HL. 2015. Population structure of mitochondrial genomes in Saccharomyces cerevisiae. BMC Genomics. 16(1):451. doi:10.1186/s12864-015-1664-4.

Yang L-L, Tang S-K, Huang Y, Zhi X-Y. 2015. Low Temperature Adaptation Is Not the Opposite Process of High Temperature Adaptation in Terms of Changes in Amino Acid Composition. Genome Biol Evol. 7(12):3426–3433. doi:10.1093/gbe/evv232.

Fig 1

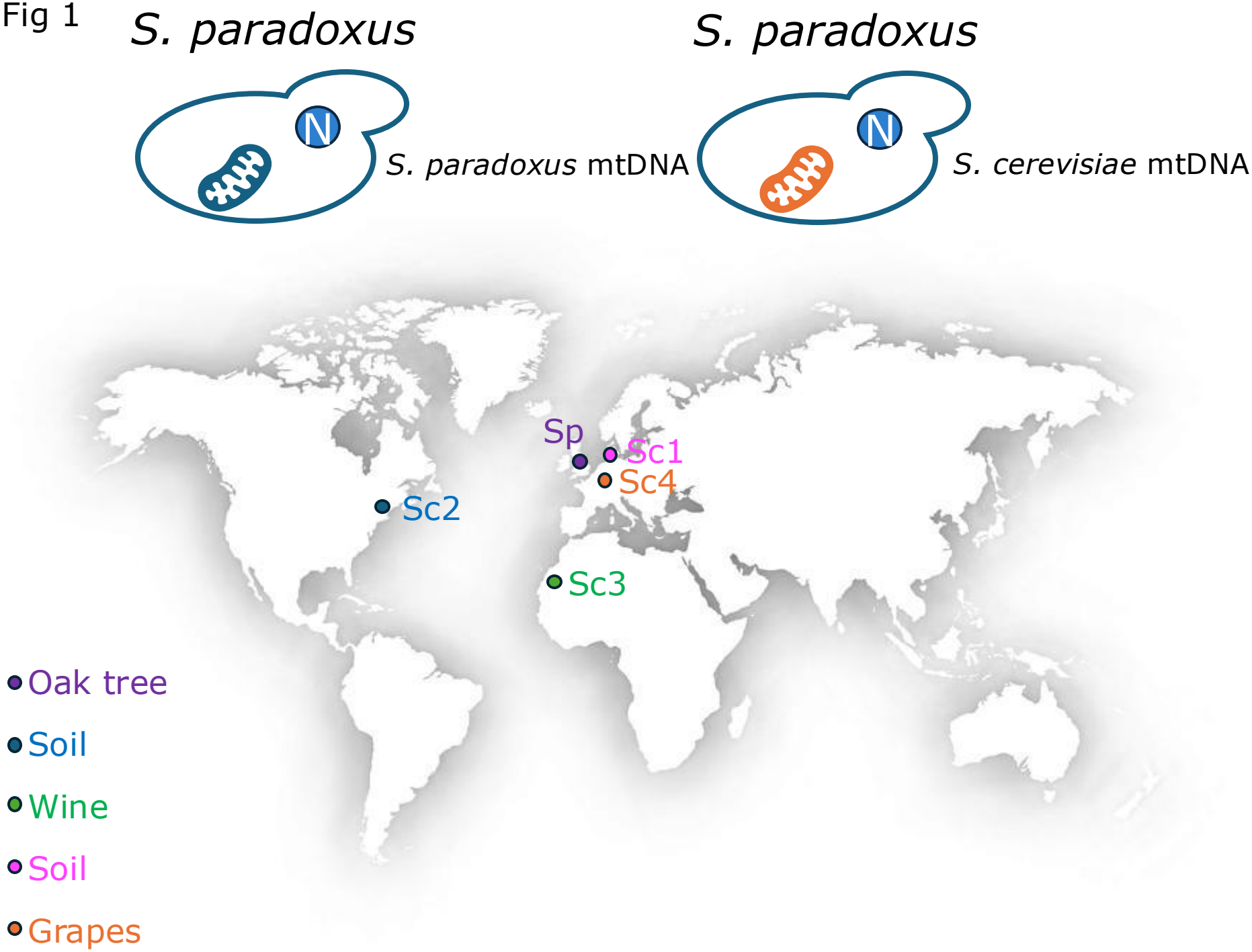
S. paradoxus
N
S. paradoxus mtDNA
S. paradoxus
N
S. cerevisiae mtDNA
Sp
Sc1
Sc4
Sc2
Sc3
Oak tree
Soil
Wine
Soil
Grapes

Fig 2A

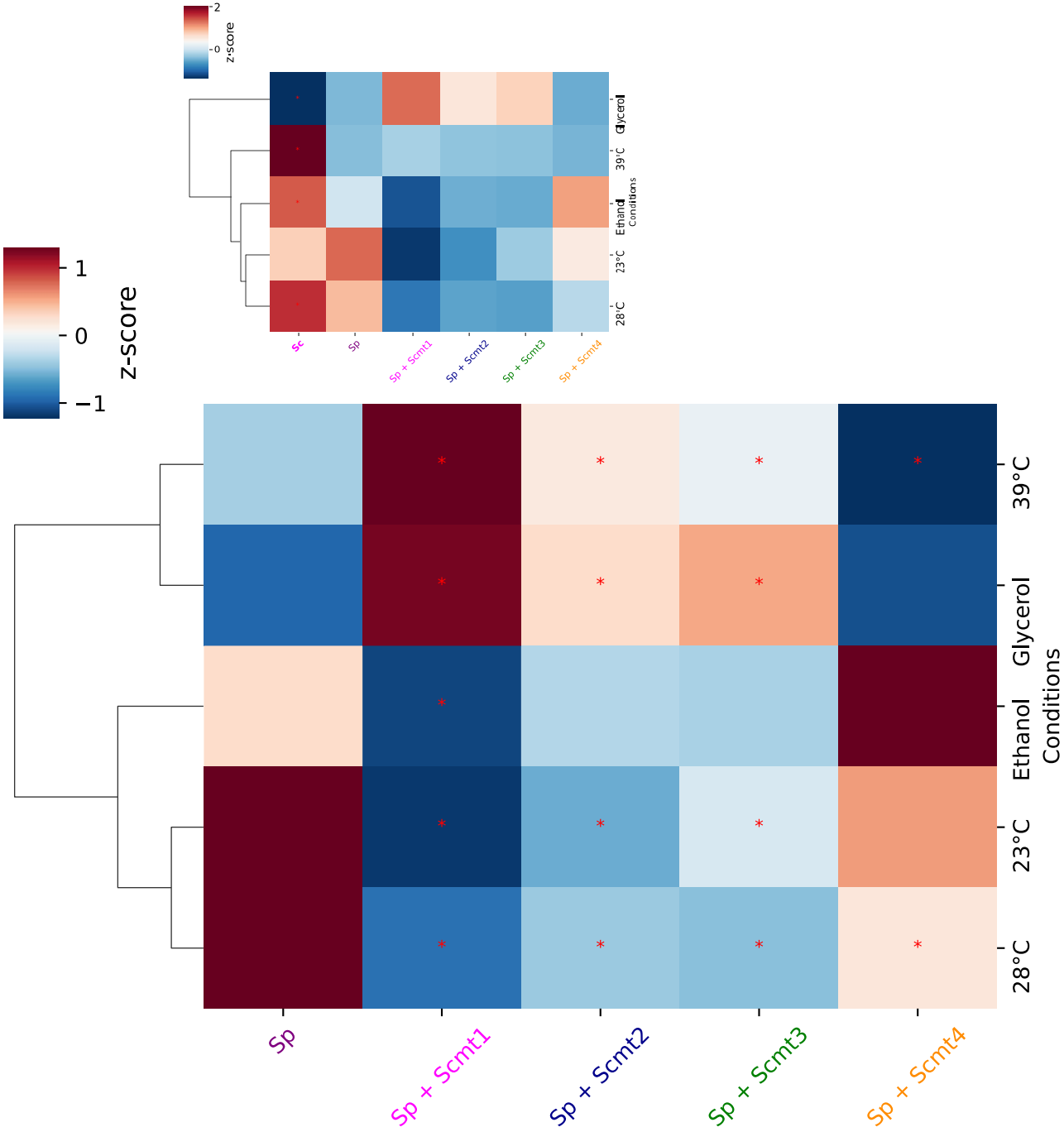
z-score
1
0
−1
Sp
Sp + Scmt1
Sp + Scmt2
Sp + Scmt3
Sp + Scmt4
28°C
23°C
Ethanol
Glycerol
39°C
Conditions

Fig 2B

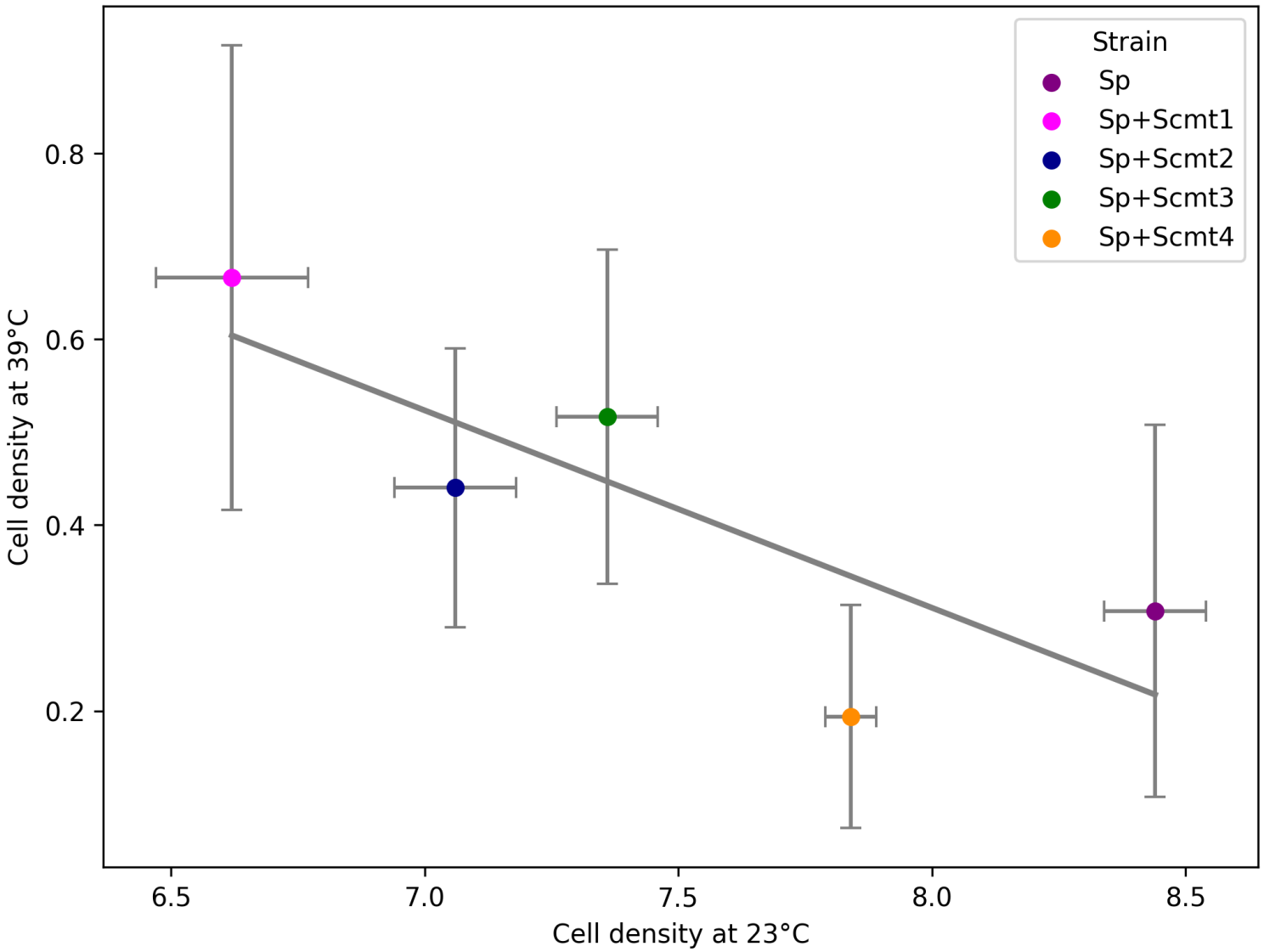
Strain
Sp
Sp+Scmt1
Sp+Scmt2
Sp+Scmt3
Sp+Scmt4
0.8
0.6
0.4
0.2
Cell density at 39°C
6.5
7.0
7.5
8.0
8.5
Cell density at 23°C

Fig 2C

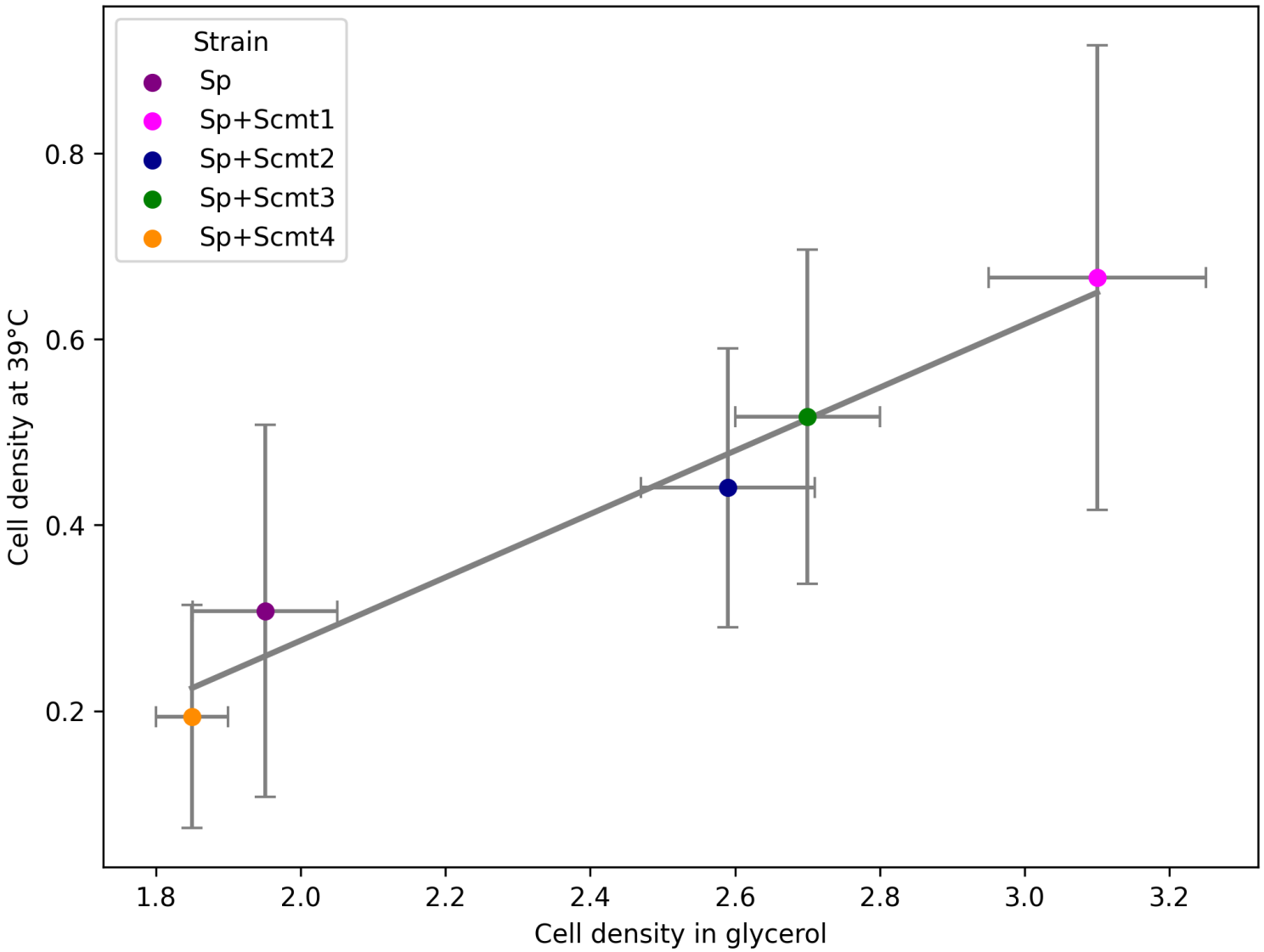
Strain
Sp
Sp+Scmt1
Sp+Scmt2
Sp+Scmt3
Sp+Scmt4
0.8
0.6
0.4
0.2
Cell density at 39°C
1.8
2.0
2.2
2.4
2.6
2.8
3.0
3.2
Cell density in glycerol

Fig 2D

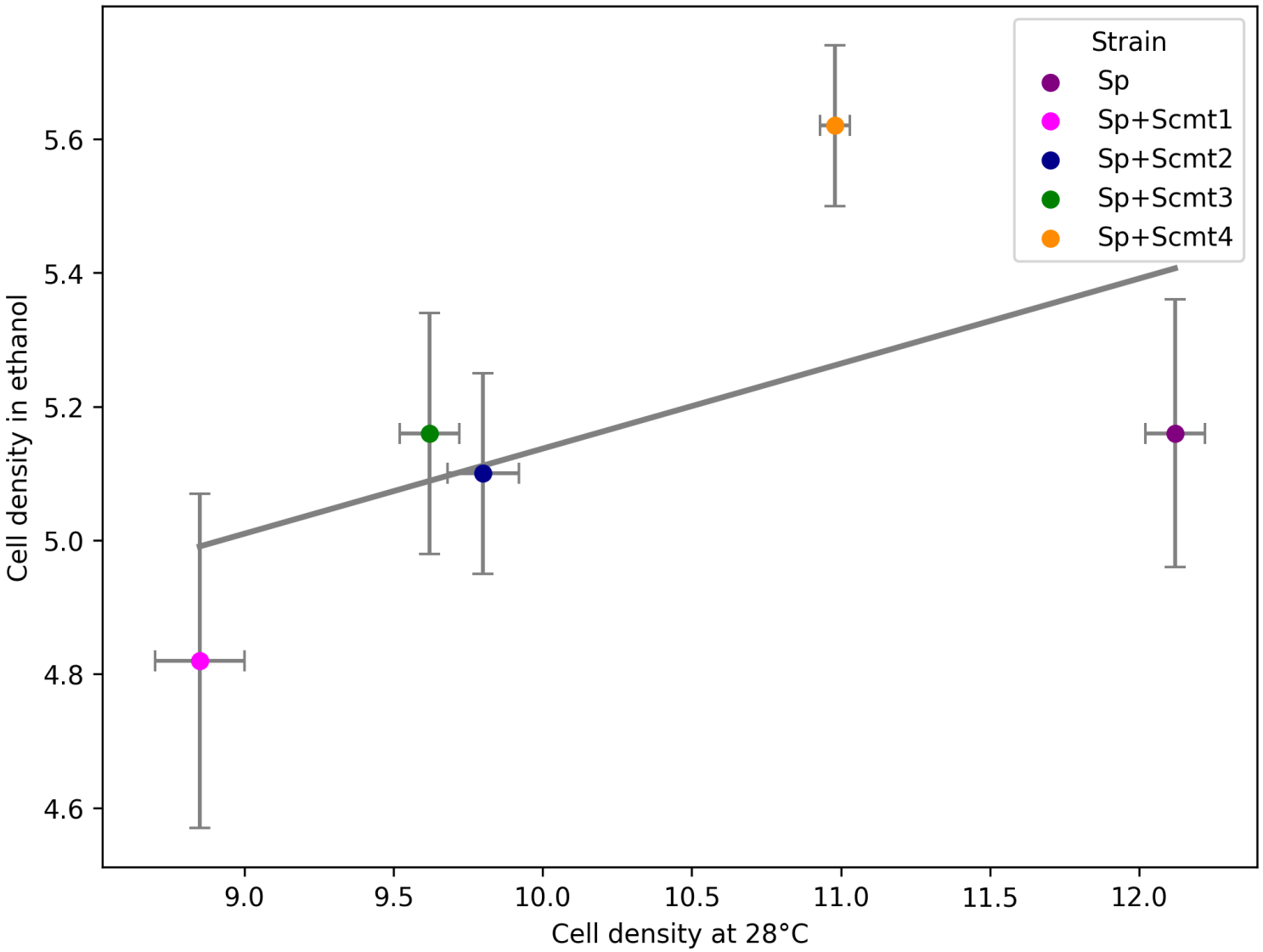
Strain
Sp
Sp+Scmt1
Sp+Scmt2
Sp+Scmt3
Sp+Scmt4
Cell density in ethanol
5.6
5.4
5.2
5.0
4.8
4.6
9.0
9.5
10.0
10.5
11.0
11.5
12.0
Cell density at 28°C

Fig 3A

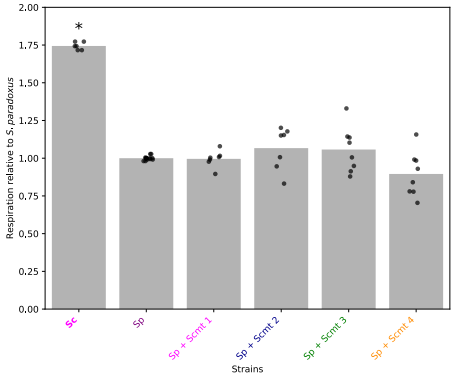
2.00
1.75
1.50
1.25
1.00
0.75
0.50
0.25
0.00
*
Respiration relative to S. paradoxus
sc
Sp
Sp + Scmt 1
Sp + Scmt 2
Sp + Scmt 3
Sp + Scmt 4
Strains

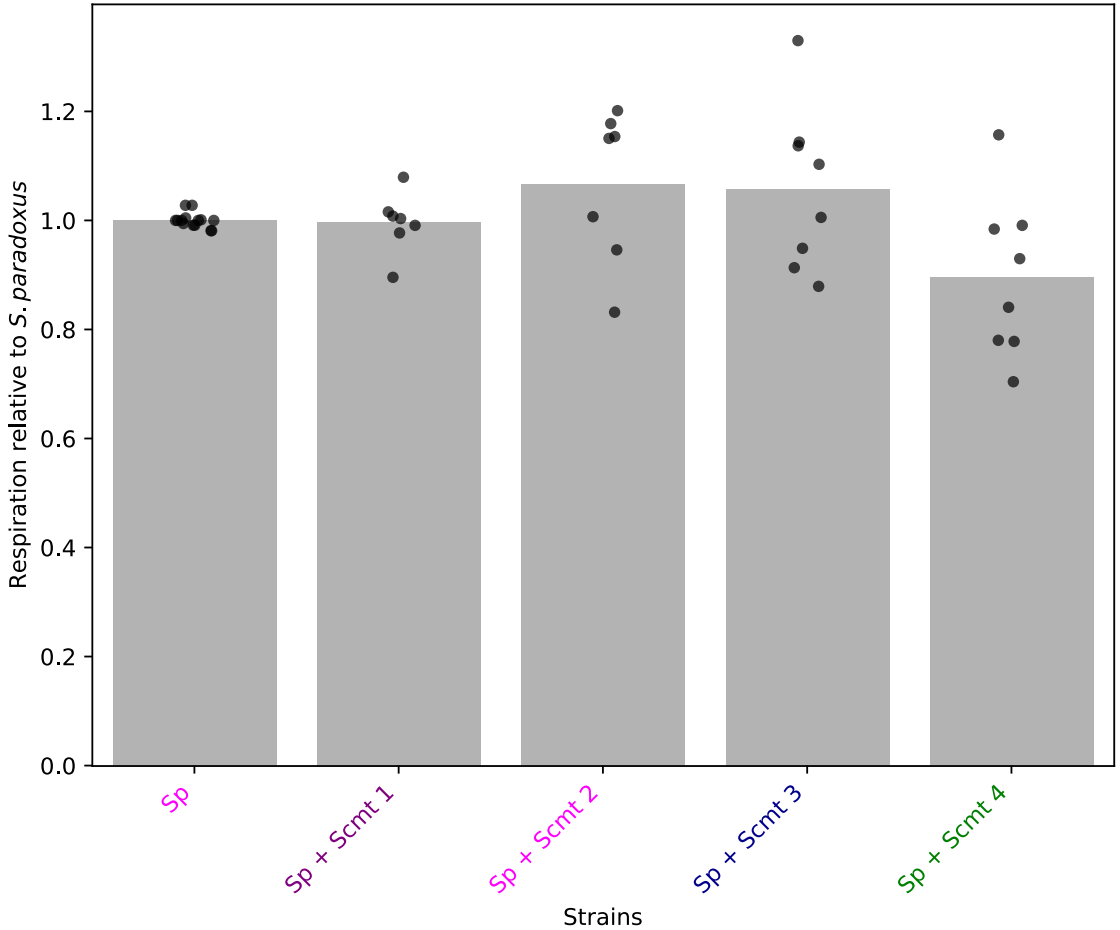
1.2
1.0
0.8
0.6
0.4
0.2
0.0
Respiration relative to S. paradoxus
Sp
Sp + Scmt 1
Sp + Scmt 2
Sp + Scmt 3
Sp + Scmt 4
Strains

Fig 3B

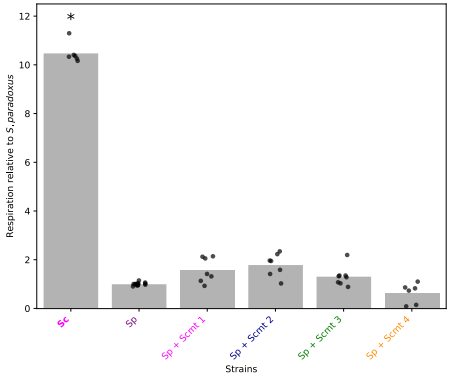
Respiration relative to S. paradoxus
Strains
Sc
Sp
Sp + Scmt 1
Sp + Scmt 2
Sp + Scmt 3
Sp + Scmt 4

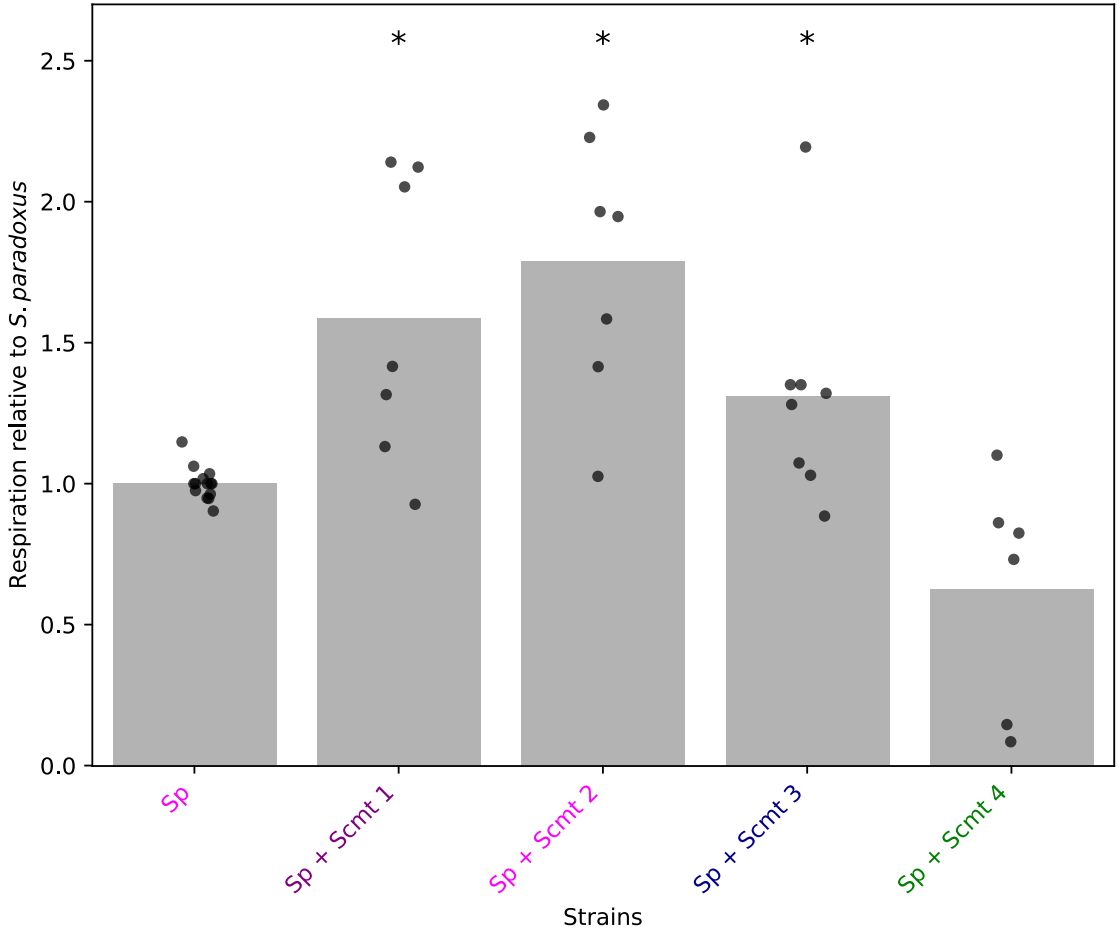
Respiration relative to S. paradoxus
0.0
0.5
1.0
1.5
2.0
2.5
*
*
*
Sp
Sp + Scmt 1
Sp + Scmt 2
Sp + Scmt 3
Sp + Scmt 4
Strains

Fig 4

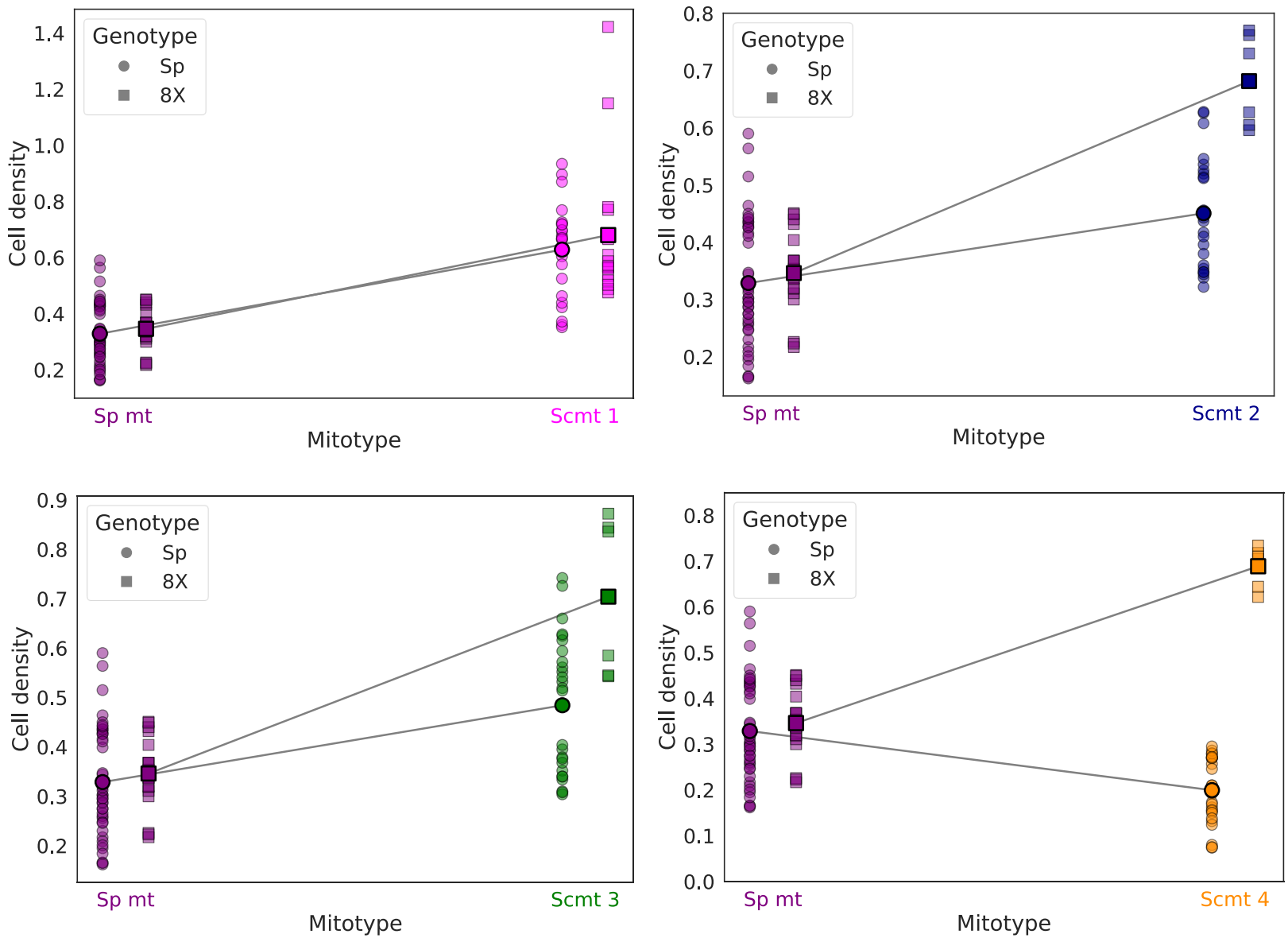
Genotype
Sp
8X
Cell density
Mitotype
Sp mt
Scmt 1
Scmt 2
Scmt 3
Scmt 4

Fig S1A

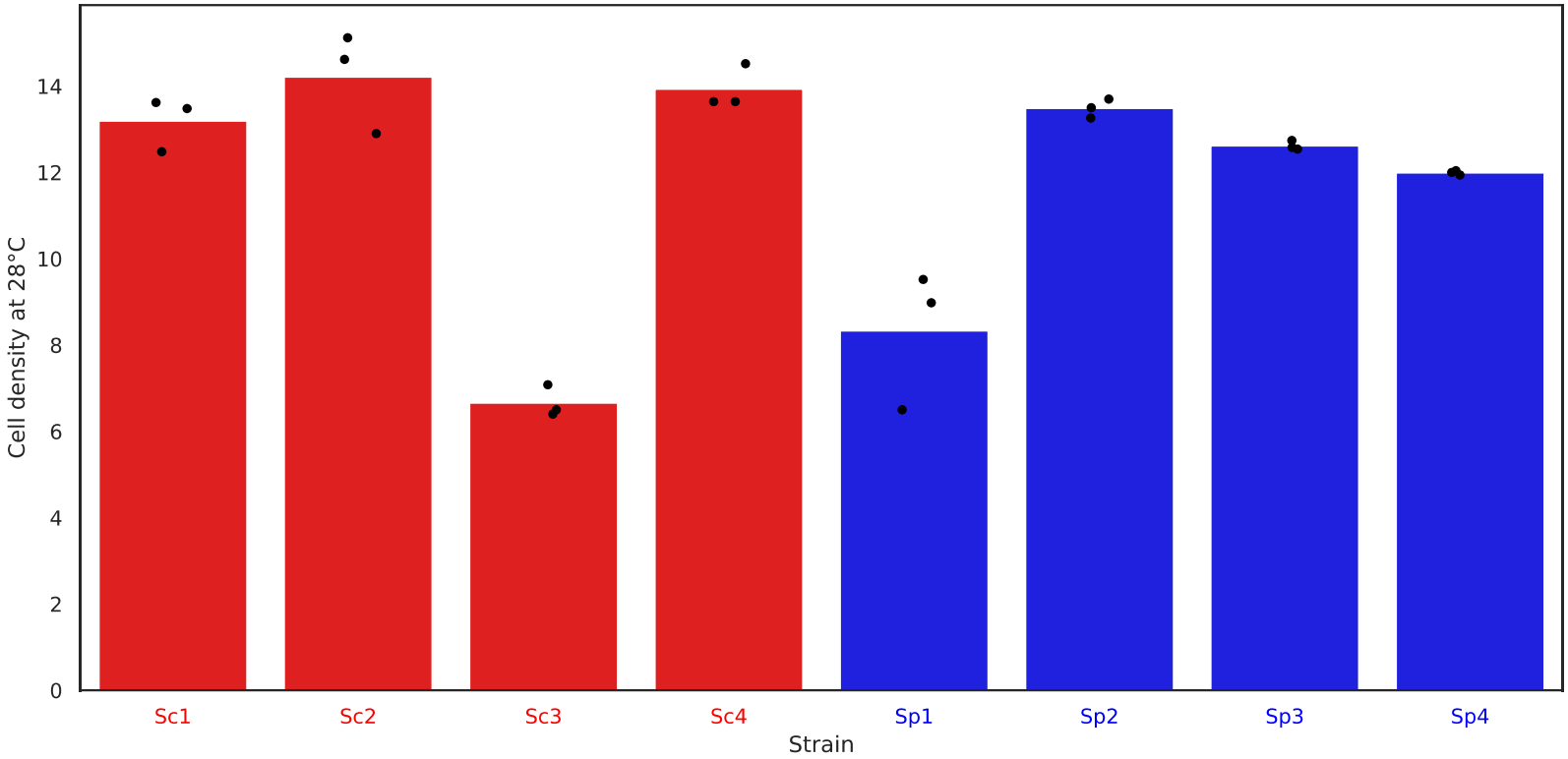
Cell density at 28°C
0
2
4
6
8
10
12
14
Sc1
Sc2
Sc3
Sc4
Sp1
Sp2
Sp3
Sp4
Strain

Fig S1B

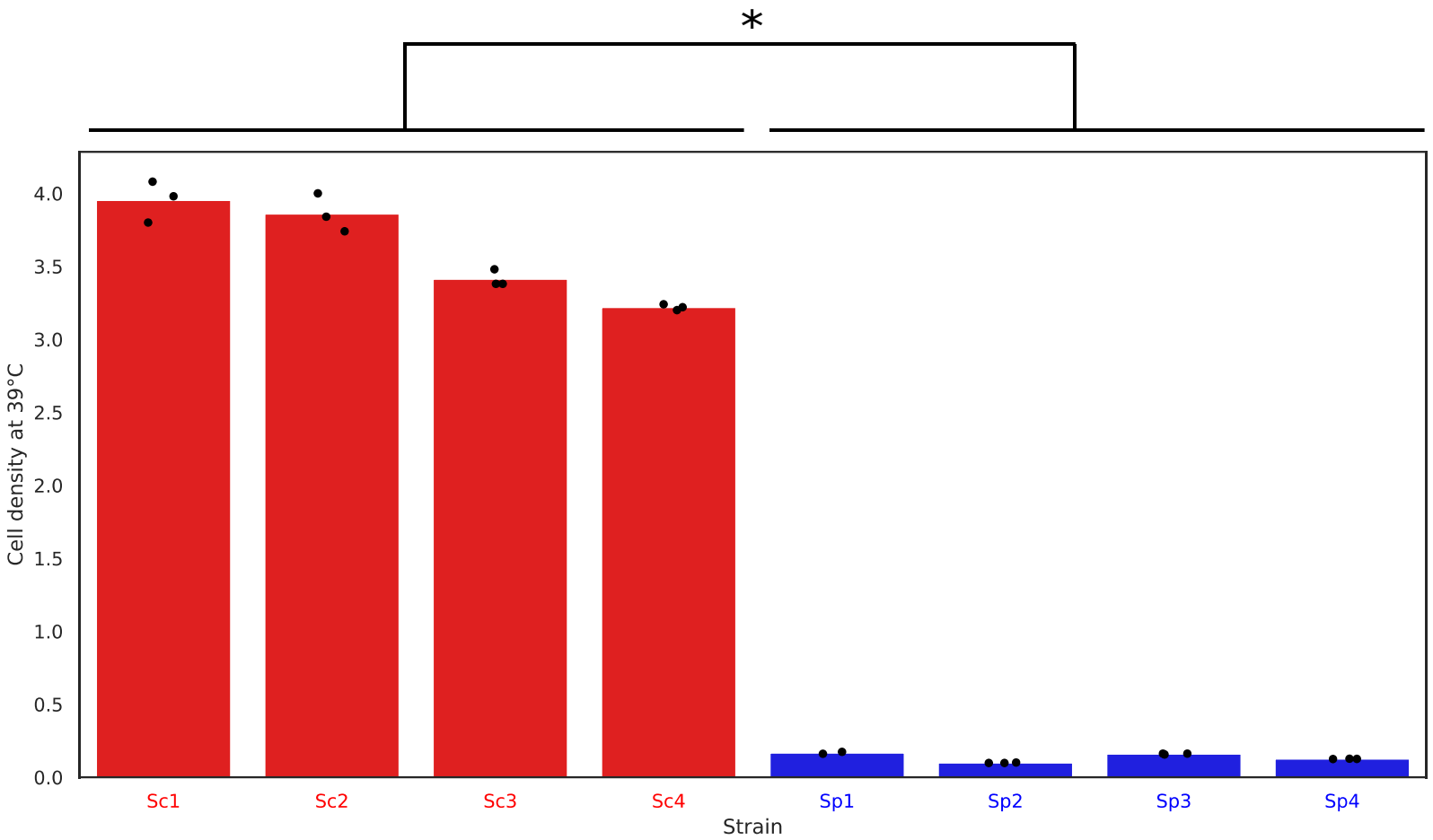
*
Cell density at 39°C
4.0
3.5
3.0
2.5
2.0
1.5
1.0
0.5
0.0
Sc1
Sc2
Sc3
Sc4
Sp1
Sp2
Sp3
Sp4
Strain

Fig S2A

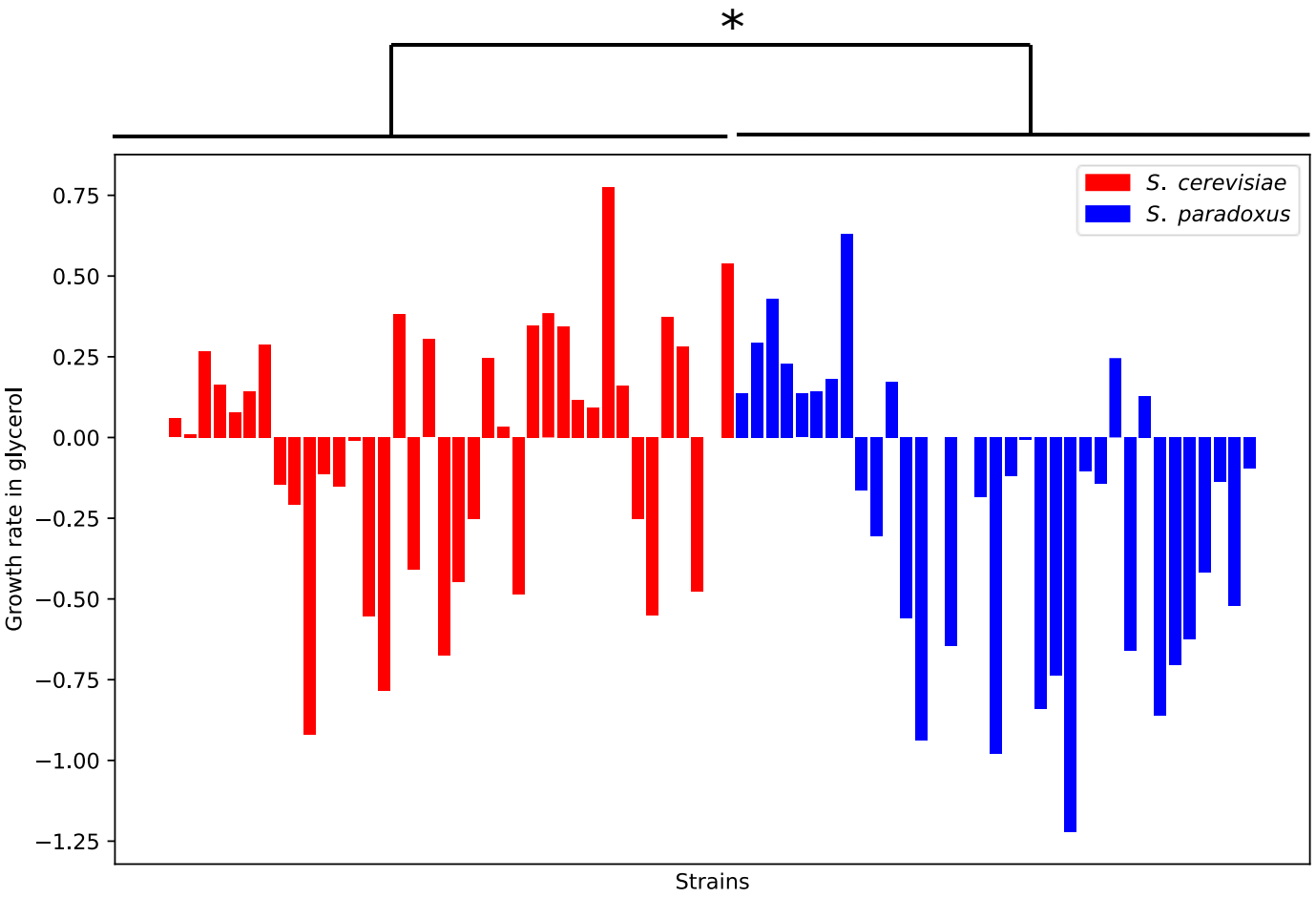
*
S. cerevisiae
S. paradoxus
0.75
0.50
0.25
0.00
−0.25
−0.50
−0.75
−1.00
−1.25
Growth rate in glycerol
Strains

Fig S2B

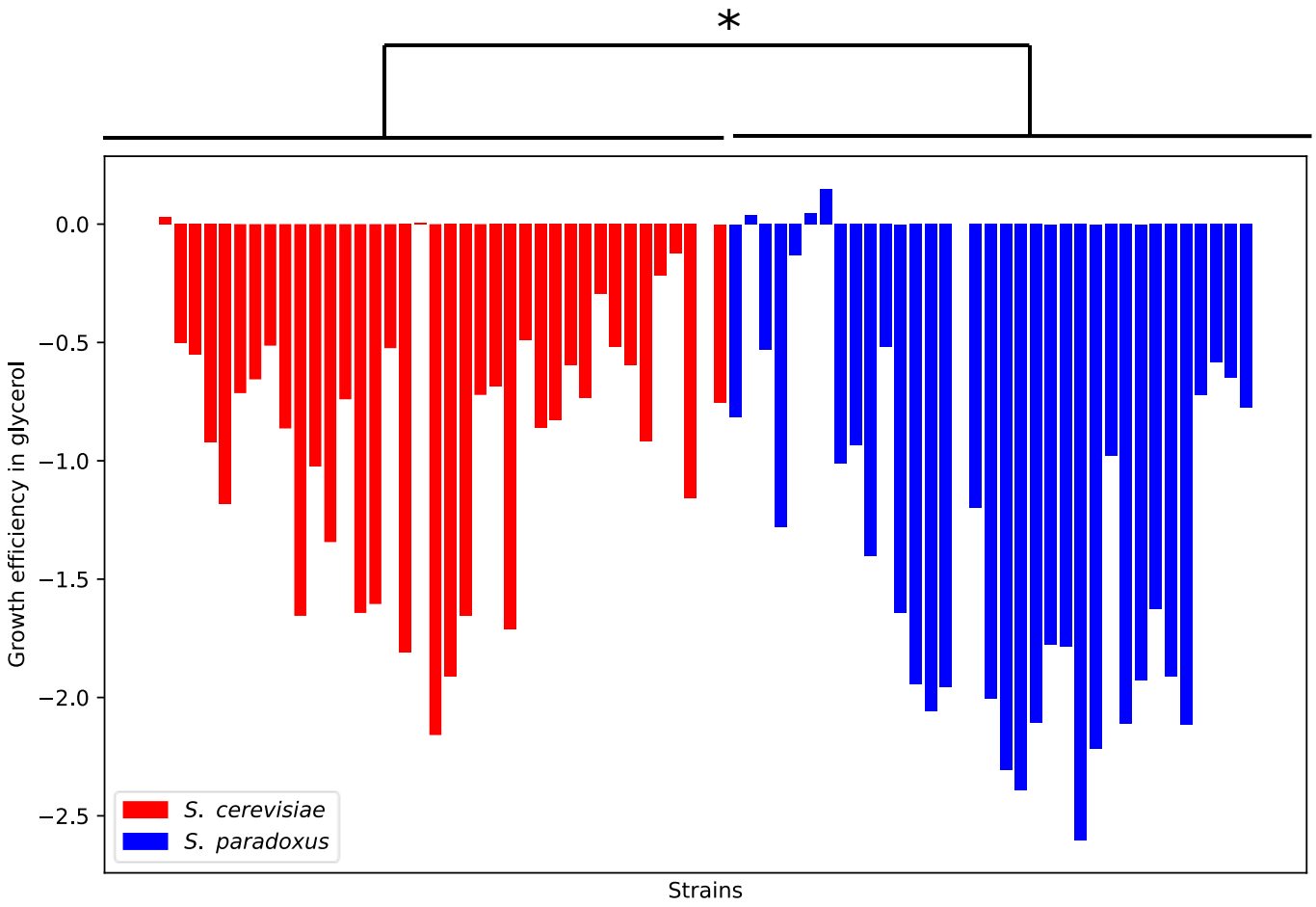
*
0.0
−0.5
−1.0
−1.5
−2.0
−2.5
Growth efficiency in glycerol
S. cerevisiae
S. paradoxus
Strains

Fig S3

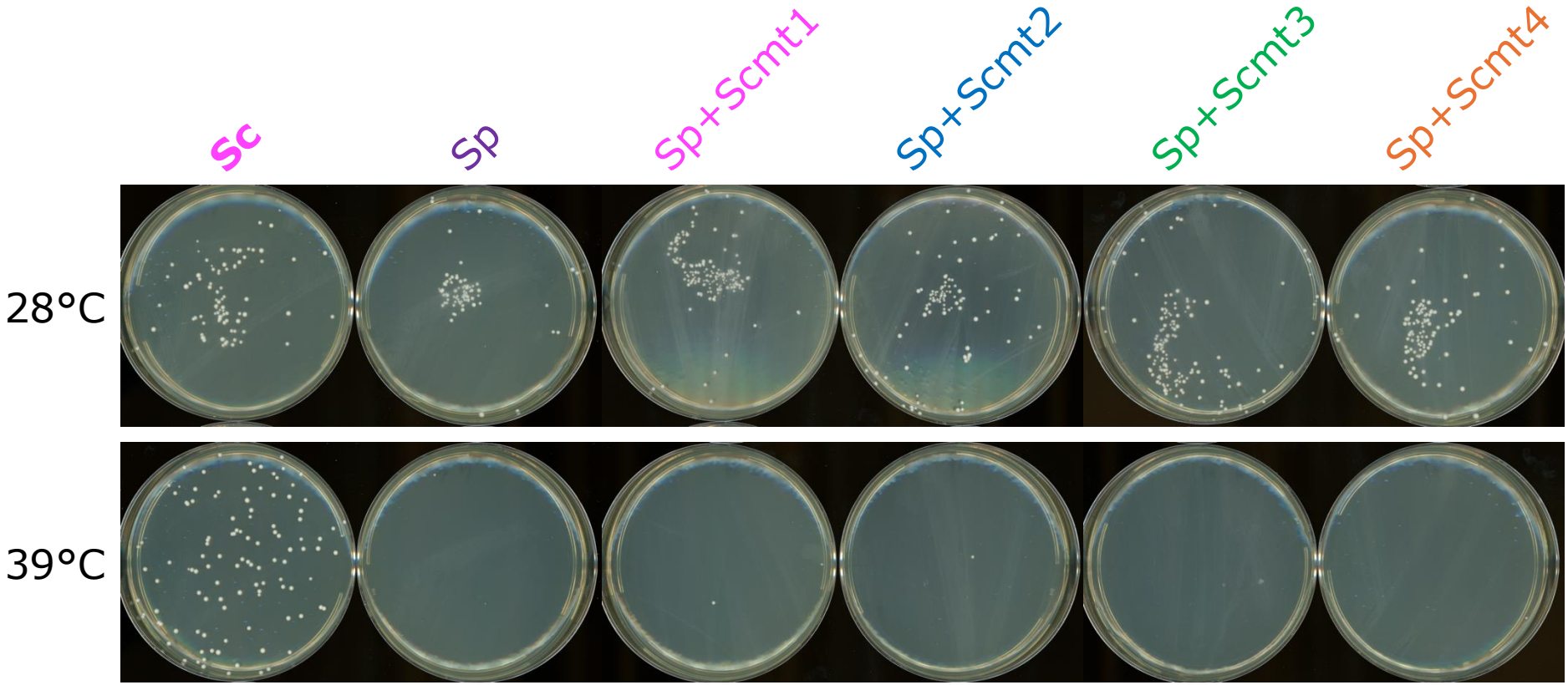

Fig S4

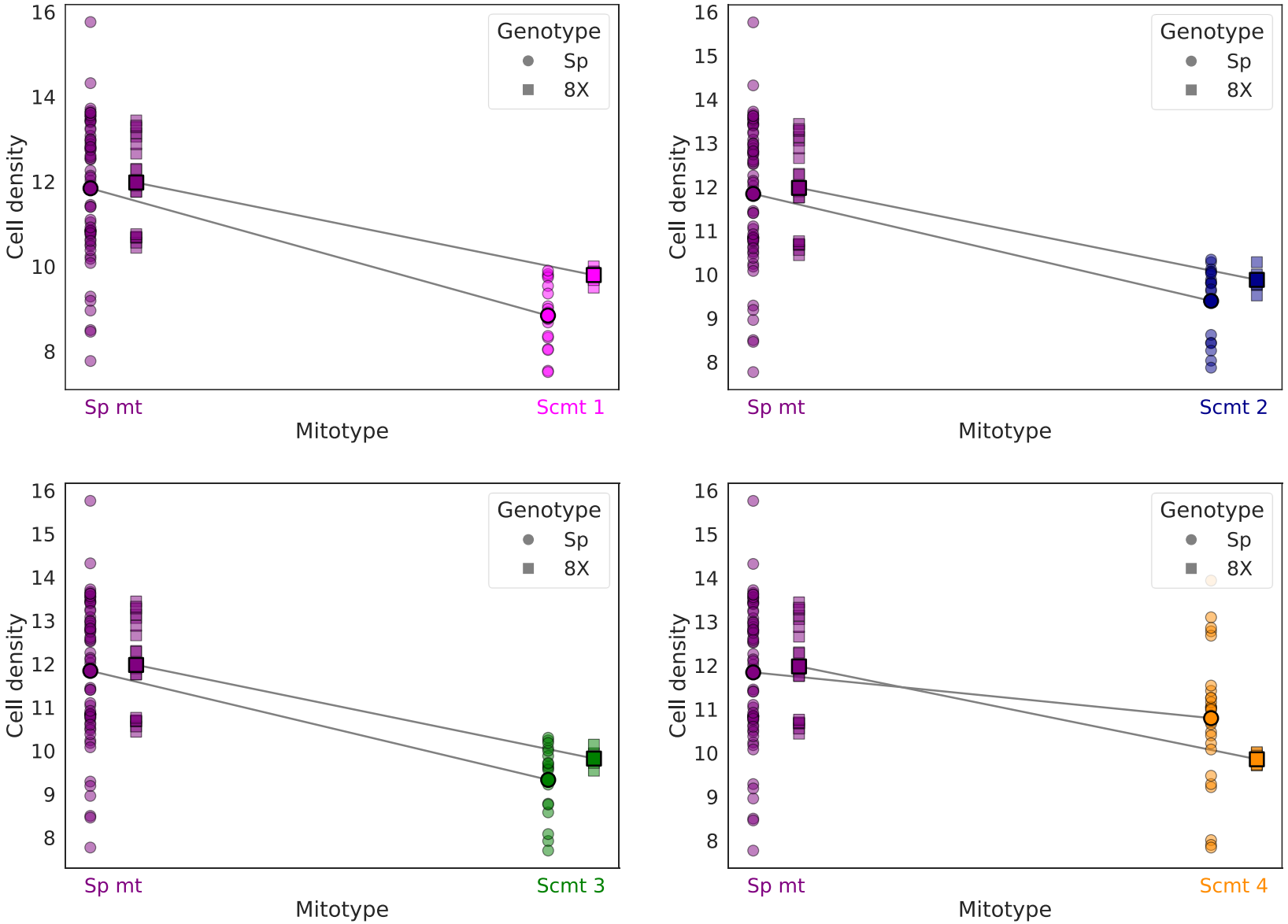
Genotype
Sp
8X
Cell density
Mitotype
Sp mt
Scmt 1
Scmt 2
Scmt 3
Scmt 4
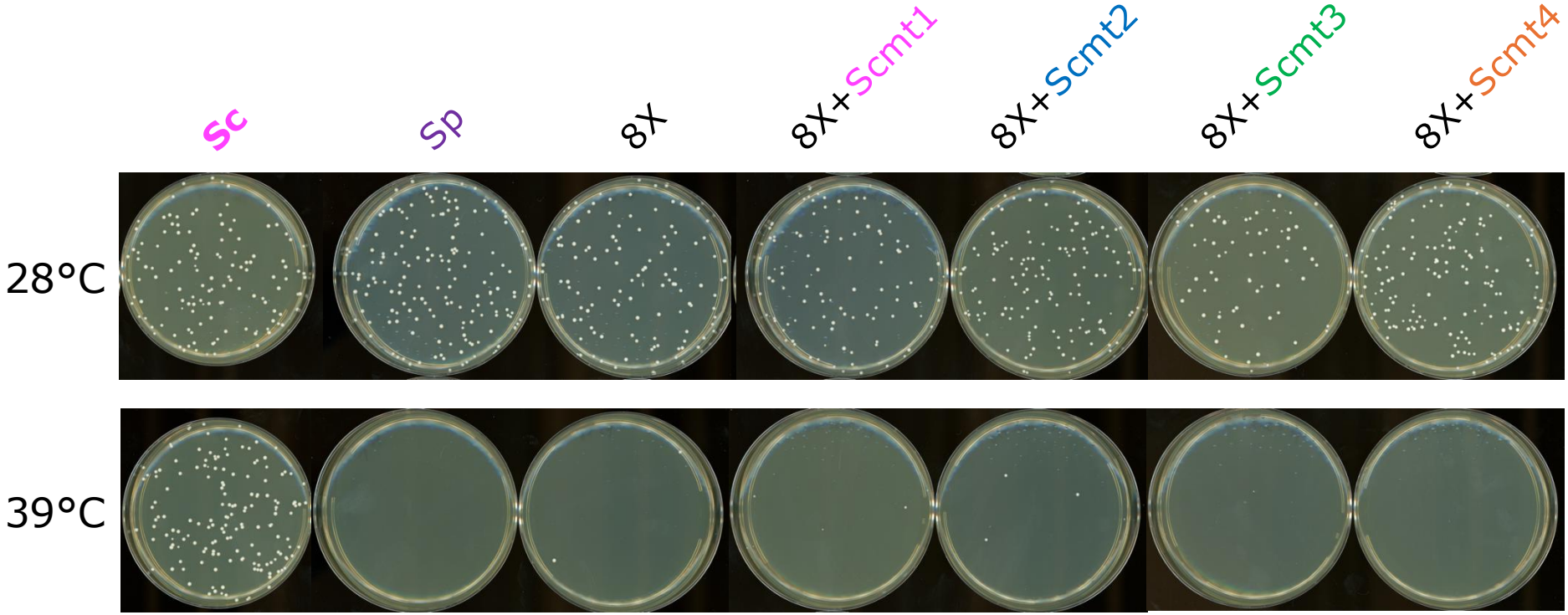
Fig S5